Journal of Hydrology 633 (2024) 131020

Contents lists available at ScienceDirect

Journal of Hydrology

journal homepage: www.elsevier.com/locate/jhydrol

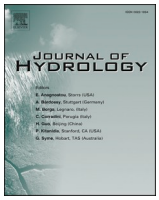

Research papers

Assessing the impact of drought on water cycling in urban trees via *in-situ* isotopic monitoring of plant xylem water

A-M. Ring [a,b,*], D. Tetzlaff [a,b,c,*], M. Dubbert [d], J. Freymueller [a], C. Soulsby [c]

[a] Department of Ecohydrology & Biogeochemistry, Leibniz Institute of Freshwater Ecology and Inland Fisheries, Berlin, Germany
[b] Department of Geography, Humboldt University Berlin, Berlin, Germany
[c] Northern Rivers Institute, School of Geosciences, University of Aberdeen, UK
[d] Research Area 1 "Landscape Processes", Leibniz Institute for Agricultural and Landscape Research, Müncheberg, Germany

ARTICLE INFO

Keywords:
Urban ecohydrology
Stable water isotopes
Drought
In-situ isotopes
Plant water use
Urban green space

ABSTRACT

Urban trees are an integral part of sustainable cities. They regulate the local microclimate and enhance the urban water cycle. Increasing periods of drought can impair urban trees by affecting their water uptake, transpiration and growth patterns. In this study, we used a multi-proxy approach to assess how non-irrigated urban trees react to changing water supply throughout the full vegetative period of 2022 including a major drought in Berlin, Germany. Our work focused on individual mature trees in an urban green space; examining daily mean *in-situ* isotopes in plant xylem water (δ_{xyl}) while also monitoring vegetation dynamics via sap flow, stem increments, LAI, as well as groundwater, and soil moisture at different depths. The monitoring period was characterised by a spring with average precipitation inputs, followed by an extremely dry period from July until mid-August, then a gradual rewetting from the end of August until October. At the beginning of the growing period, changes in the ecohydrological dynamics of the investigated maple and birch trees were high with increases in stem size and LAI, but also decreasing soil moisture. In spring, δ_{xyl} signatures were high in both trees, with the effect more marked in the maple hinting at a dependence of δ_{xyl} on species specific-storage effects and a distinct start of transpiration. During summer, drought stress was apparent in the ecohydrological fluxes of the monitored trees in the reduction of stem growth, LAI, midday water potential and soil moisture. Yet sap flow rates were relatively stable and tree transpiration maintained. We noted a midsummer enrichment of δ_{xyl} in both species. Most importantly, the measured δ_{xyl} signatures were isotopically in the range of deep soil waters and groundwater implying that deeper sources were sustaining the trees' water supply during the drought. We also detected fractionation of δ_{xyl}, which is possibly induced by heterogenous water uptake strategies and biochemical processes in the tree xylem, including CH_4 transport. Our results suggest that urban trees rely on deep water supply and internal storage during drought. We conclude urban trees and shrubs with shallow root development would be more vulnerable to dry summers with a particular threat during future accelerated summer droughts combined with insufficient autumn rewetting causing deep soil layers to dry out.

1. Introduction

Urban trees and woodlands are important in cities across the world for amenity (Dwyer et al., 1991; Bolund & Hunhammar, 1999; Roy et al., 2012), nature conservation and local biodiversity increase (Grimm et al., 2008; Kowarik, 2011). They also provide important ecosystem services to improve health for residents (Shashua-Bar et al., 2011; Willis & Petrokofsky, 2017) and water security (Bichai & Cabrera Flamini, 2018; Aboelnga et al., 2019). Through increasing infiltration rates and enhancing groundwater recharge, urban woodland overall enhances the urban water cycle (McGrane, 2016) and positively affects the urban heat balance through increased evapotranspiration (ET) rates (Livesley et al., 2016). Urban green spaces, can thus regulate a cities' microclimate through mitigation of urban heat island effect through cooling via latent heat production (Oke, 1982).

Urban areas are especially subject to climatic warming (Wouters et al., 2017; Bastin et al., 2019; Dodman et al., 2023) and the frequency and severity of droughts has increased in Europe since 2018 (Bastos et al., 2021; Paton et al., 2021; Smith et al., 2022; Conradt et al., 2023). This threatens urban trees: moisture stress has induced reduced growth,

* Corresponding authors at: Department of Ecohydrology, Leibniz Institute of Freshwater Ecology and Inland Fisheries, Berlin, Germany.
E-mail addresses: ann-marie.ring@igb-berlin.de (A.-M. Ring), doerthe.tetzlaff@igb-berlin.de (D. Tetzlaff).

https://doi.org/10.1016/j.jhydrol.2024.131020
Received 16 September 2023; Received in revised form 19 February 2024; Accepted 20 February 2024
Available online 6 March 2024

lowered ET rates and even led to tree mortality following dry years in Berlin and other European cities (Gillner et al., 2020; Rötzer et al., 2021).

Studies on these interlinkages and water cycling through the soil–-plant-atmosphere continuum in urban areas are still rare and hence, these processes are less understood in cities compared to other environments (forests, croplands etc.) (Ehleringer et al., 2016; Oswald et al., 2023). In general, on-site long-term observations of ET are rare, especially in urban dwellings were ET estimates are complex because of the heterogeneity of green spaces and building structures that have an effect on shading, heat storage and funnelling of winds(Arnfield, 2003; Saher et al., 2020; Duarte Rocha et al., 2022). In particular, urban tree ET has shown contrasting patterns in its diurnal and seasonal cooling effects depending on the trees' location, species, size and water supply (Meili et al., 2021; Tams et al., 2023).

The use of stable water isotopes can help to understand water cycling through trees in the soil–plant-atmosphere continuum (SPAC) (Tetzlaff et al., 2015). Tracer methods now enable tracking of water at a high spatial and temporal resolution within the water cycle (Sprenger et al., 2017; Sprenger et al., 2019) across varied geographic regions (Yakir & Sternberg, 2000; Dubbert & Werner, 2018; Tetzlaff et al., 2021). However, research pertaining to the fluxes and cycling across the SPAC in urban settings is still limited (Soulsby et al., 2014; Kuhlemann et al., 2021; Marx et al., 2022). Only recently has it become possible to monitor tree xylem water isotope dynamics *in-situ* "in real time" with several monitoring studies producing reliable long-term data at high resolution (up to sub-daily) (Mennekes et al., 2021; Seeger & Weiler, 2021; Kübert et al., 2022; Kühnhammer et al., 2022; Landgraf et al., 2022). In addition to isotope tracing, monitoring of ecohydrological processes like sap flux, biomass accumulation (via shrink and swell patterns of dendrometer data), soil moisture and leaf area index (LAI) provides further insights on urban tree water cycling (Ponte et al., 2021; Rocha & Holzkämper, 2023; Stevenson et al., 2023). Finally, combining stable water isotopes with more general ecohydrological monitoring helps understand the sources of water in root uptake, (urban) ET and the general water partitioning through trees (Deurwaerder et al., 2020; Kuhlemann et al., 2021; Fabiani et al., 2022; Landgraf et al., 2022).

Here, we focus on trees in an urban green space in Berlin, NE Germany, building on previous work on using isotopes in urban ecohydrology in this city (Gillefalk et al., 2021; Kuhlemann et al., 2021; Landgraf et al., 2022; Marx et al., 2022). In 2022, the year of this study, Germany suffered another exceptional summer drought (Meinert et al., 2022), also affecting the vegetation productivity of NE Germany (Conradt et al., 2023). This drought was still impacting soil moisture profiles in NE Germany in 2023 (UFZ Leipzig, 2023). Further, the prolonged drought caused high urban tree mortality in Leipzig, Germany (~150 km distance to Berlin) (Haase & Hellwig, 2022). It is projected that such drought periods will be more frequent in the future (Rakovec et al., 2022; IPCC, 2023). Indeed, Berlin lately implemented the need to optimise green and open spaces for more cooling in their new urban development plan (StEP Klima 2.0 from SEnSBW, 2022). Overall, a better understanding of the ecohydrology of urban green trees is urgently needed.

In this context, the overarching aim of this study was to use a multi-proxy approach to investigate the daily ecohydrological fluxes and water cycling of urban trees during the entire growing period of 2022 (including a major summer drought). Our work focused on individual mature trees in an urban green space; examining daily mean *in-situ* isotopes in plant xylem water (δ_{xyl}) while also monitoring vegetation dynamics via sap flow, stem increments, LAI, groundwater levels and soil moisture at different depths.

Our specific research questions were:

i) What is the seasonal variability in the ecohydrology of urban trees (in terms of leaf out, potential soil water sources, transpiration and stem increment growth)?
ii) Can continuous monitoring of plant xylem water isotopes (δ_{xyl}) help understand the sources of urban tree water uptake?
iii) Is there any evidence that urban trees become water stressed during summer droughts?

Thus, our work contributes new knowledge on the water cycling of urban trees in drought years, providing evidence-base for stakeholders towards a more resilient and sustainable management of urban green spaces.

2. Study site

We conducted our experiment in an urban setting in the SE of Berlin, Germany (Fig. 1). Berlin covers an area of 891 km^2, with a population of 3.85 million (Amt für Statistik Berlin-Brandenburg, 2023; Fig. 1A). The city is located on the North European Plain with a flat topography that consists of > 100 m of Quaternary deposits (Limberg & Thierbach J., 2002). These sand and gravel deposits form the Warsaw-Berlin glacial spillway that characterises the Geology of Berlin (Limberg et al., 2007). The climate is continental temperate with long-term (1991–2020) mean annual rainfall of 579 mm and mean annual air temperatures of 9.6–10.7 °C (DWD, 2023b). The region is becoming more drought-sensitive, being warmer and drier in recent years compared to the reference period from 1981 to 2010 (ibid.). In 2022, Berlin only received 403 mm of rainfall and during 2018 (when a major drought occurred in central Europe), annual precipitation was only 420 mm (DWD, 2023a). Across the city, residential areas and streets comprise ~ 59 %, vegetation cover ~ 34 % (forests, parks, agriculture) and surface waters make ~ 7 % (SenUVK, 2019a).

The study site is located at Leibniz-Institute of Freshwater Ecology and Inland Fisheries (IGB), roughly 220 m north of Lake Müggelsee (Berlin's largest lake) (Fig. 1a). The surrounding district (Fig. 1A) has large areas of green and blue space. The site is characterised by forest (40 %), residential areas and roads (38 %), water bodies (12 %) and public green space (0.06 %; SenUVK, 2019b). The study site was spread with mature trees (~30–100 years old) and extensive dry grassland surrounded by brick buildings of a former 19th century water works. Within a 100 m radius of the study site center (Fig. 1b), different types of non-irrigated urban green spaces cover the premises, including grassland (49 %), shrubs (8 %) and tree canopy (17 %), as well as grey infrastructure like buildings (10 %), and streets, semi-permeable, sealed pathways and parking spaces (16 %). The experiment focused on one tree-dominated area (Fig. 1b), which is characterized by maple, birch, lime, oak and black locust trees. We selected one dominant Norway maple tree (*Acer platanoides*) with a stem diameter of 560 mm (measured in April 2022) and height of ~ 16 m and one dominant silver birch tree (*Betula pendula*) with a stem diameter of 490 mm (measured in April 2022) and a height of ~ 12 m. The genus *Acer* comprises 20 % of Berlin street trees (SenMVKU), but has shown significant growth decline in drought years (Gillner et al., 2014).

In addition to the tree site, we studied a grassland area 15 m away. This was covered by several grass species (e.g. *Arrhenatherum elatius, Lolium perenne*) and herbs (e.g. *Achillea millefolium, Trifolium pratense*) of 30–50 cm height, mowed twice a year. The soils at the study site are sandy regosols (GeoportalBerlin, 2015), which reflect anthropogenic impacts through existing debris, sandy materials and a shallow humus layer (roughly 8 cm deep). In the 1st meter of depth, soils at the study site were overall sandy (more than 94 % of fractions > 0.063 mm). The groundwater level was around 2.25 m deep and affected by lake water extracted via bank filtration.

3. Data and methods

3.1. Monitoring

The study period was from April 1st to November 1st 2022 (i.e. a full

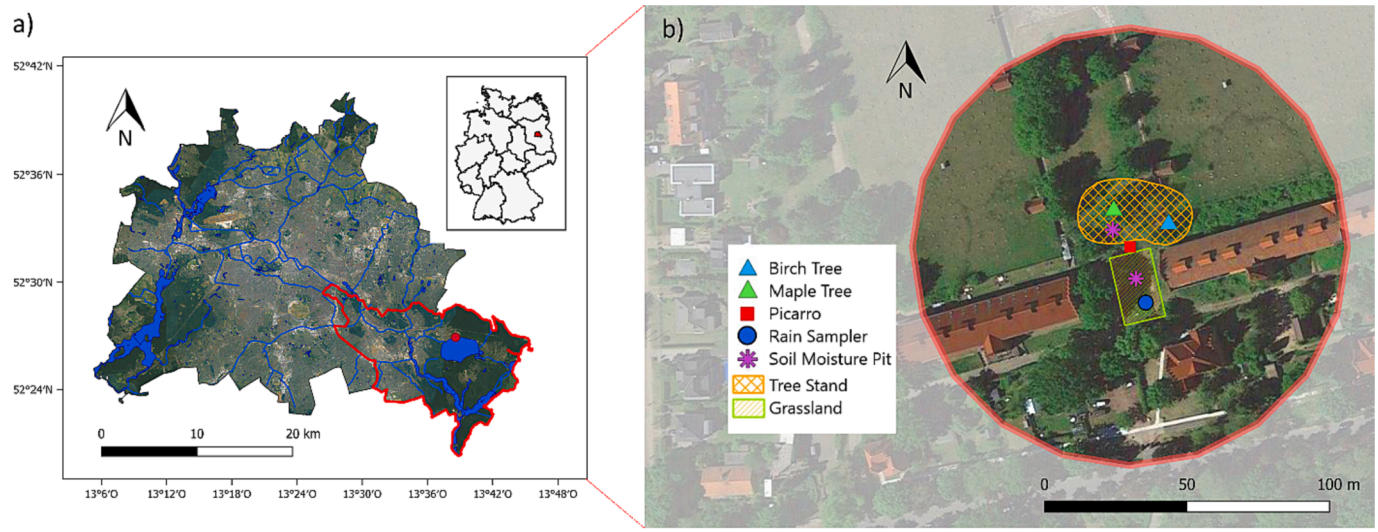

Fig. 1. Location of Berlin within Germany and map of Berlin (a); and the study site at IGB Berlin (b): the tree site with Acer platanoides and Betula pendula and grassland (with soil water isotope measurements only); and installations of sap flow (in both trees) and soil moisture measurements and sampler for precipitation isotopes (75 m radius from CRDS in center). (Basemap: Google Satellite).

vegetative period). Climate data (air temperature, precipitation amount, wind speed and direction, relative humidity, air pressure, global radiation) were accessed from the rooftop of IGB ~ 300 m away. On-site, we measured precipitation at the open grassland (tipping bucket raingauge, 0.2 mm/tip, precision ± 3 % of total rainfall; AeroCone® Rain Collector, Davis Instruments, Hayward, USA) and relative humidity at the maple tree stem at 2 m height in south-east direction (Vaisala Humicap® Humidity and temperature probe HMP155, accuracies: ±1 %RH (0 … 90 % RH) ± 1.7 %RH (90 … 100 %RH)). Both were recorded with a CR800 Datalogger (Campbell Scientific, Inc. Logan, USA) logging every 15 min. On-site temperature was recorded every 5 min with BetaTherm 100K6A1IA Thermistors T107 (Campbell Scientific, Inc. Logan, USA; tolerance ± 0.2 °C (over 0°–50 °C)) with a CR300 Datalogger (Campbell Scientific, Inc. Logan, USA). All precipitation and temperature data were verified against data from the German Weather Service (DWD) of the "Berlin-Marzahn" station (DWD, 2023a) (Station ID: 420), ~12 km north of the study site.

Daily precipitation isotopes were sampled manually with a HDPE deposition sampler (100 cm^2 opening; Umwelt-Geräte-Technik GmbH, Müncheberg, Germany). Samples with precipitation < 1 mm were discarded to limit evaporation effects. Additionally, we sampled precipitation with an autosampler (ISCO 3700, Teledyne Isco, Lincoln, USA) at a 24 h interval which was placed ~ 350 m away. The autosampler bottles were filled with a paraffin oil layer > 0.5 cm in thickness (after IAEA/GNIP, 2014) to avoid evaporative effects.

Groundwater isotope samples were taken weekly with a submersible pump (COMET-Pumpen Systemtechnik GmbH & Co. KG, Pfaffschwende, Germany) from a well on IGB grounds ~ 300 m away.

For isotope analysis of the liquid water samples at the IGB laboratory all samples were filtered (0.2 um cellulose acetate) and decanted into 1.5 mL glass vials (LLG LABWARE) and analysed by cavity ring-down spectroscopy (CRDS; L2130-i, PICARRO, INC., Santa Clara, CA). For calibration we used four standards for a linear correction function. They were referenced against three primary standards of the International Atomic Energy Agency (IAEA). For quality-checking and averaging multiple analyses of each sample the ChemCorrect software (Picarro, Inc.) was applied to screen for interference from organics. Results were expressed in δ-notation with Vienna Standard Mean Ocean Water (VSMOW). Analytical precision was 0.05 ‰ standard deviation (SD) for $\delta^{18}O$ and 0.14 ‰ SD for $\delta^{2}H$.

Stable isotopes of xylem water (δ_{xyl}), later on termed as plant water isotopic signatures, were measured *in-situ* real-time and sequentially

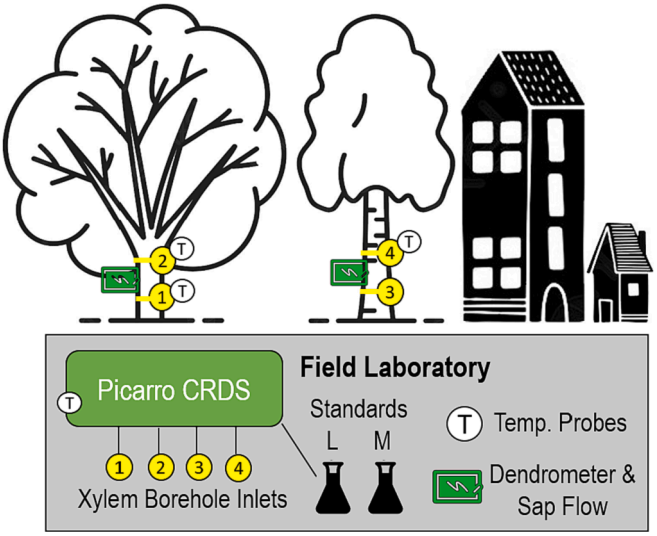

Fig. 2. Conceptual diagram of the general in-situ plant xylem water isotope (δ_{xyl}) measuring setup with the birch tree growing near a building. Numbers refer to different tube inlets for δ_{xyl} from boreholes.

(Fig. 2). Measurements were performed using the same instrument type as above. At each tree, two stem boreholes were drilled through the full stem horizontally (stem borehole equilibration) at 1.5 m and 2.5 m height to capture possible variation within heights and effects of travel times within the trees stems. The method of stem borehole equilibration was developed and tested in several studies in recent years (Beyer et al., 2020; Marshall et al., 2020; Kühnhammer et al., 2022); see Landgraf et al., 2022 for a detailed description of the method at our study site.

For this study, δ_{xyl} measurements started on 25.04.2022, two weeks after installation, to exclude the start data with potential wounding signals (cf. Landgraf et al., 2022). Each tube inlet (Fig. 2) was sampled for 30 min in 1 Hz resolution, and then sampling switched automatically to the next tube inlet. Individual xylem inlets were measured every ~ 3 h, including calibrations and auxiliary measurements into the monitoring sequence. The first 12 min of data after switching inlets were always discarded to avoid memory effects and only data with stable values was used (i.e. ranges of 3 ‰ for $\delta^{2}H$ and 0.8 ‰ for $\delta^{18}O$). The

sample flow rate was at 0.04 L min^{-1}.

The measurement sequences of the CRDS were checked daily, to detect technical problems in regard to e.g. condensation or wounding effects. Data was discarded when any biased measurement was identified in the respective tube until normal sequences have established. For example, we could not use the δ_{xyl} data of the maple borehole at 2.5 m height as it showed overall unstable and unreasonably high measurements from wounding, which occurred simultaneously with extremely high CH_4 signals at the multiport valve. The CH_4 originated from the borehole and hindered stable measurements of δ_{xyl} with CRDS. The boreholes of maple at 1.5 m and birch at 1.5 m height also showed higher CH_4 signals than the usual tropospheric concentration (~2 ppm; (Khair et al., 2017)) just after switching valves, but the δ_{xyl} measurements reached stable values afterwards.

For later conversion of δ_{xyl} measurements into liquid water isotope values, temperature probes were installed inside the borehole membranes (fine PFA-sealed resistance thermometers (Pt100, HSRTD, Omega Engineering, Norwalk, USA; tolerance: ±0.15 to 0.35C (over 0 to 100 °C)) and logged with a CR800 Datalogger (Campbell Scientific, Inc. Logan, USA) logging mean values every 15 min from second-resolution data. By combining δ_{xyl} with temperature data from each borehole we derived the values for all *in-situ* boreholes of temperature dependent equilibrium fractionation from vapour to liquid with the correction formulated by Majoube (1971):

$$\alpha = exp\frac{a\left(\frac{10^6}{T_k^2}\right) + b\left(\frac{10^3}{T_k}\right) + c}{1000}, \quad (1)$$

where α is the isotopic fractionation factor, Tk is the temperature (in K), and a, b, and c are empirical parameters that vary depending on the isotopologue.

All values of δ_{xyl} isotopic compositions are given for the liquid phase and relative to Vienna Standard Mean Ocean Water (VSMOW) so all isotopic values can be compared with each other. CRDS measurements were calibrated automatically with two standards after every 3 loops of xylem measurements (liquid values: light: $\delta\ ^2H$ −73.623 ‰/ $\delta\ ^{18}O$ −10.522 ‰; heavy: $\delta\ ^2H$ 16.74 ‰/ $\delta\ ^{18}O$ 1.53 ‰). To correct for isotopic offsets and vapour concentration dependency, water vapour concentrations in the headspace of the glass containers were measured and linear regressions of temperature dependency slopes added. We included regular checking for stable values of both standards to avoid headspace depletion.

Further, we took destructive samples of stable isotopes of bulk soil water at monthly intervals from April until October 2022. Bulk soil water sampling was conducted at the tree stand and at the open grassland site (Fig. 1b). Always three replicate samples were collected at 0–5, 5–10, 10–20, 20–40 and 40–70 cm depth. We utilized a sampling ring for depths up to 10 cm; below that, we employed a soil auger with a diameter of 4 cm. Samples were contained in stable bags (CB400-420siZ, WEBER Packaging GmbH, Güglingen, Germany) and zip-locked airtight. The samples underwent 48 h of equilibration before analysis. For further details consult Kleine et al. (2020). Soil water isotopes were analysed using the direct equilibrium method outlined by Wassenaar et al. (2008). For analysis, the vapour of the soil water isotopes in the bags was extracted and analysed with a Los Gatos off-axis integrated cavity output spectroscopy (OA-ICOS) triple water-vapour isotope analyser (TWIA-45-EP, Los Gatos Research, Inc., San Jose, CA, USA). For correction, two 10 mL standard water samples were used three times during every measuring routine (light: $\delta\ ^2H$ −73.623 ‰/ $\delta\ ^{18}O$ −10.522 ‰; heavy: $\delta\ ^2H$ 20.89 ‰/ $\delta\ ^{18}O$ 1.80 ‰). The vapor in each bag was measured for 8–10 min to ensure a stable plateau using the method by Marx et al., (2022): Gradient and quantile filters were used to identify the plateau and generate a reliable mean. Standards were utilized for drift control throughout the measurement and over the year, as well as to convert from the vapor phase back to the liquid phase.

Line-conditioned excess (short lc-excess) (see Landwehr & Coplen, 2006) was calculated for local evaporative effects. Lc-excess describes the deviation of the sample from the local meteoric water line (LMWL):

$$lc - excess = \delta^2H - a{\cdot}\delta^{18}O - b, \quad (2)$$

where *a* is the slope and *b* the intercept of the weighted isotopic composition of the local precipitation. The LMWL was calculated by amount-weighted least square regression (Hughes & Crawford, 2012) from daily precipitation isotopes measured at IGB during the whole year of 2022.

In order to fully assess the dynamics in the SPAC of the urban trees we added extensive monitoring of its ecohydrological components: sap flow, stem increment growth, potential evapotranspiration, soil moisture, groundwater levels, LAI and plant water potential. We monitored sap flux and the stem circumference of the maple and birch tree at breast height (1.3 m). At the maple tree, two sap flow sensors (SFM-4, Umwelt-Geräte-Technik GmbH, Müncheberg, Germany; ±0.1 cm/hr heat velocity precision) were installed at the north and south side of the tree stem. Additionally, we placed different sap flow meters (SFM1 instrument, ICT International, Australia): one at northwestern side of the maple and three surrounding the birch treés stem (north, northwest and south). All sap flow sensors work according to the heat ratio method by Marshall (1958). Dendrometers (DR Radius Dendrometer, Ecomatik, Dachau, Ger170; accuracy max. ± 4.5 % of the measured value (stable offset)) were installed to measure the stem diameter dynamics and monitor stem increment growth (in mm) at high temporal resolution. Daily potential evapotranspiration (PET) was estimated using meteorological data from the rooftop of IGB and the FAO Penman–Monteith method (Allen, 1998) with "R"-Package "Evapotranspiration" (Guo, 2022). We were interested in the general dynamics of PET rather than absolute values during the vegetative period to see whether there was a limit on the trees meeting atmospheric moisture demand, therefore, both sap flow rates [$cm^3\ d^{-1}$] and PET were normalised by mean values with feature scaling.

Volumetric soil water content and soil temperature were measured at two soil pits, one underneath the maple tree and the other at a grassland nearby (Fig. 2b). We placed soil moisture temperature probes (SMT-100, Umwelt-Geräte-Technik GmbH, Müncheberg, Germany) at 5 depths ranging from 5 cm to 70 cm (precision of ± 3 % for volumetric soil water content and ± 0.2 °C for soil temperature). Both soil pits consisted of sandy soils at all depths (over 94 % of fractions > 0.063 mm). Estimation of soil water storage as volumetric percentage from the total (1000 mm) soil profile for comparison among sites (in mm water column in the first meter) was attained by weighting measured volumetric soil moisture corresponding to each depth. Depending on the number of sensors, the profile was divided into segments which were assumed to be represented by each sensor. Sap flow, stem increments and soil moisture were logged at 15 min intervals using a CR800 Datalogger (Campbell Scientific, Inc. Logan, USA).

Groundwater level was monitored with an automatic datalogger (groundwater level probe) in one well on IGB's grounds ~ 300 m away from the study site. LAI was measured once a month the same day when destructive soil sampling was carried out. We measured LAI underneath both trees at 2 m height with a plant canopy analyzer (LAI 2000, Li-cor, Inc., Lincoln, NE, USA) at a constant location taking the mean of 3 replicates. A tree's LAI is positively correlated to sap flow rates as leaf stomatas compensate water fluxes (Oren et al., 1999). Therefore, LAI can be used as a proxy for stand transpiration (Zhang et al., 2018). Additionally, we added twig water potential measurements at both trees during midday twice a month from June until November with a Scholander pressure chamber instrument (Model 1000, PMS Instrument Company, Albany, OR, USA; 0.5 % accuracy).

3.2. Statistical analysis

For statistical data analysis of differences and correlations of the obtained dataset we performed several statistical tests. First we tested normality of all datasets with the Shapiro-Wilk test (Shapiro & Wilk, 1965). For the non-normally distributed data of daily median δ_{xyl} valueswe used non-parametric alternatives (assuming all observations were independent and random): the Wilcoxon signed-rank test for two groups (Wilcoxon, 1945) and the Kruskal-Wallis test by ranks for more than two groups (Kruskal & Wallis, 1952) and post-hoc the pairwise Wilcoxon rank sum test with Bonferroni correction (Bonferroni, 1935; Wilcoxon, 1945; Mann & Whitney, 1947). To test correlations of the non-linear daily data of precipitation characteristics, soil storage of both sites, sap flow rates, stem increment growth and LAI for both tree species we applied Spearman's rho statistic (Spearman, 1904). We averaged replicas in the timeseries of the δxyl (median), LAI and meteorological values (as means) and used these means for the statistical tests. Daily totals and mean values were calculated for high-resolution data. Monthly LAI values were linearly interpolated to daily values with tied x values handled by mean. Covariances were computed by pairwise complete observations.

4. Results

4.1. Hydroclimate

Fig. 3 shows the hydro-climatological conditions surrounding the study period. The study period (01.04.-31.10.2022) was characterised by a very dry and warm summer compared to the long-term average (1991–2020) at DWD station Berlin Marzahn. Total precipitation was 262.5 mm during the study period (long-term average: 362 mm (DWD, 2023b)). Summer rain days were rare and most summer rain events were < 5 mm with the highest rainfall event in July. More frequent summer rainfall events mainly occurred in mid-August. Most rewetting took place in September. During the warm period from May until August, relative humidity was low (mean 62.8 %), temperature was high (mean 20.8 °C; long-term average: 17.9 °C (ibid.)) and VPD exceeded 1 kPa most of the summer. The preceding summer of 2021 was less dry and warm, but 2018–2020 were exceptional years of drought impacting Berlins green spaces (Kuhlemann et al., 2021).

4.2. Ecohydrological dynamics

Monthly monitoring of LAI (Fig. 4) showed rapid changes at leaf-burst (April to May) and at leaf senescence (October to November) for both the maple and birch. LAI at both trees was highest in July and dropped in August following a dry period. Only LAI values of the maple

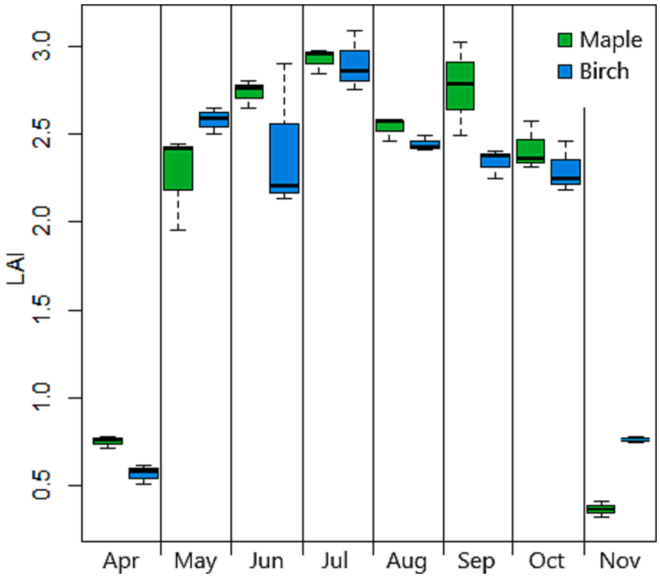

Fig. 4. Monthly LAI values of the maple and birch tree during the growing period of 2022.

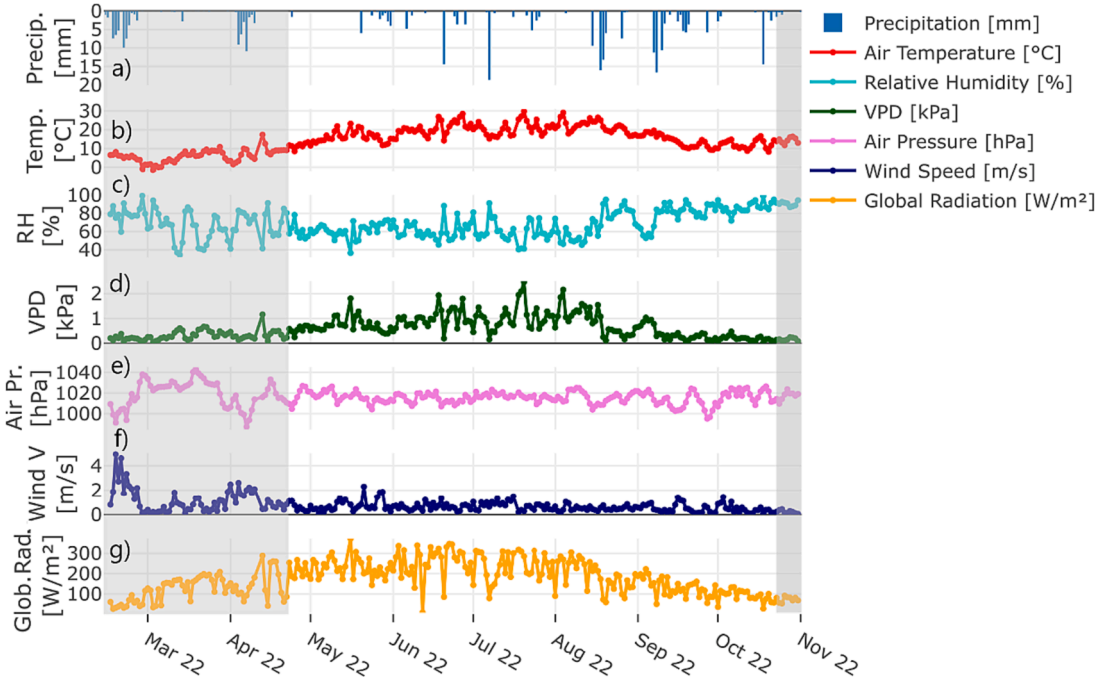

Fig. 3. Time series of daily hydroclimate variables surrounding the growing period (April – October 2022): a) precipitation [mm], b) air temperature [°C], c) relative humidity [%], d) vapour pressure deficit (VPD) [kPa], e) air pressure [hPa], f) windspeed [m/s], g) global radiation [W/m^2]. Periods before and after δ_{xyl} measurements (25.4.-20.10.2022) are shaded in grey.

tree increased again with rewetting in September, while the birch tree values continued to decrease.

Soil moisture responded to rainfall (Fig. 5a) but was generally low at both sites (Fig. 5 b,e) with the sandy upper soils being extremely dry (<5 %) for much of the summer until rewetting started in mid-August. The upper soil moisture storage rapidly responded to precipitation inputs, but quickly decreased again afterwards reflecting the low water holding capacity of sand. Only larger events in late summer increased

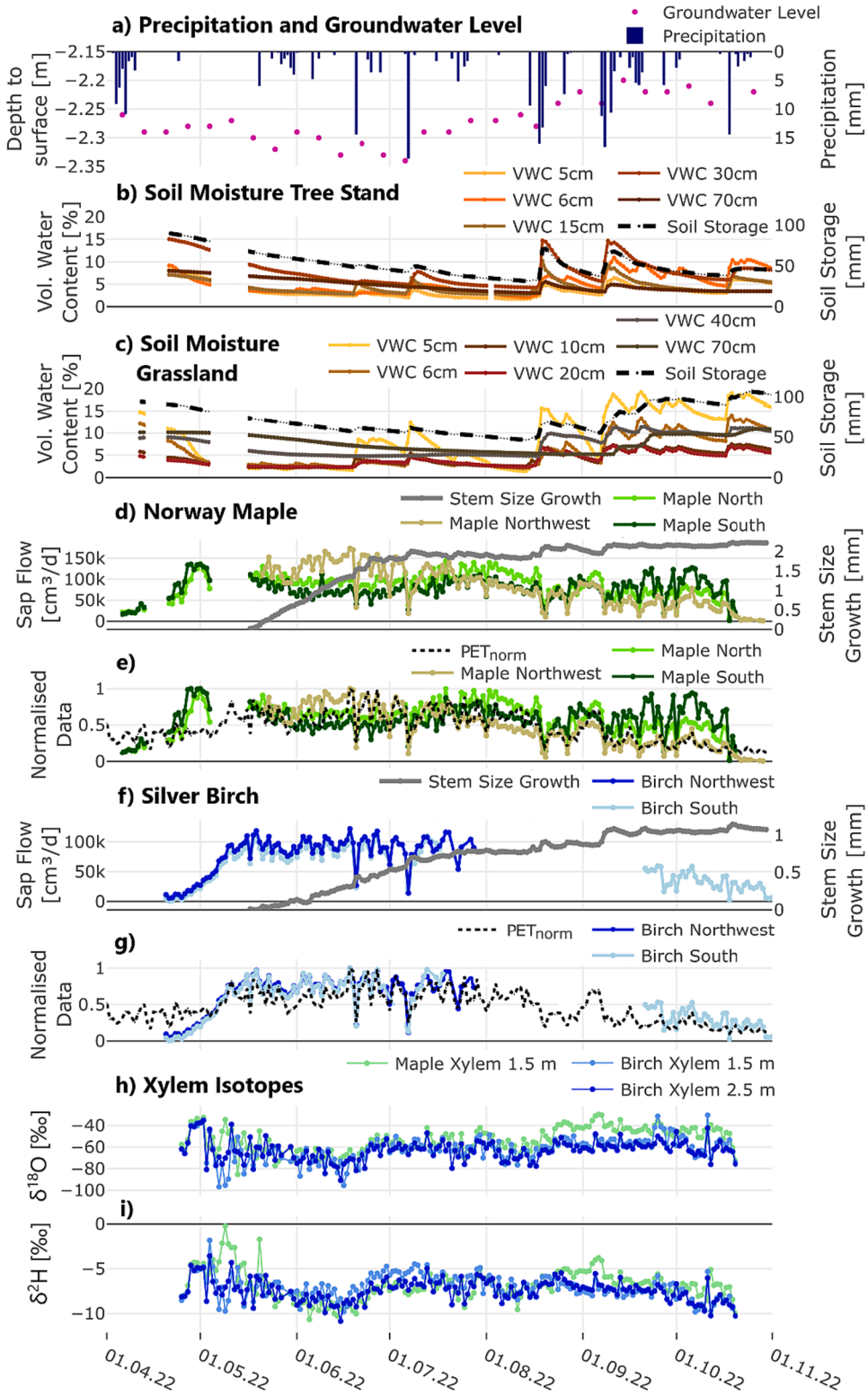

Fig. 5. Timeseries of daily precipitation and weekly groundwater level (a); daily soil moisture (at 5 depths) and soil storage in the first metre of the soil beneath tree canopy (b) and beneath the nearby grassland (c); daily sapflow and stem size growth measured for the stem-radius of the maple (d); daily normalised sap flow of the maple and potential evapotranspiration (PET_{norm})(e); daily sapflow and stem size growth measured for the stem-radius of the birch (f); daily normalised sap flow of the birch and PET_{norm} (g); daily median xylem water isotopes of δ^2H (h) and $\delta^{18}O$ (i).

the moisture content at 70 cm and groundwater levels showed limited variation (Fig. 5a) varying around 2.27 m depth (range 16 cm) throughout the study period.

Dendrometers of both trees (Fig. 5 d,f) imply that despite rapid stem increment growth in spring (Fig. S2c,d), during the drought (mid-July until mid-August) the stem diameter of both trees did not increase and sometime shrinking seemed to have occurred. After rainfall events, the stem diameters increased rapidly in August and September.

Sap flow rates of both trees (Fig. 5 c,f) increased from April to May. They briefly dropped during larger rainfall events when atmospheric moisture demand declined despite rising soil moisture after an event. Sap flow rates of the maple tree decreased for some days in late July and August when drought was most extreme (unfortunately sap flow sensors in the birch tree ceased operating in July, though one was repaired in September). For a few days in August and September, the normalised potential evapotranspiration (PET_{norm}) (index for atmospheric moisture demand) exceeded the normalised sap flow measured in the maple indicating tree water demand was not met (Fig. 5 d,g). Despite this, PET_{norm} did not exceed the measured sapflow during the dry period in July and August.

Midday water potential (ψ) (Fig. S1) was most negative from spring until summer and increased again after rewetting in August and September. Maple ψ responded to the major summer rain event on July 7 with a slight increase (the measured soil moisture in the 0.7 m deep pits decreased quickly after that event, Fig. 5).

For a more detailed understanding, we also show three selected time periods in more detail (Fig. 6). The first column of the panels shows the ecohydrological responses during the month of May in more detail. Maple sap flow rates (Fig. 6d) increased and became steady over the month. Birch sap flow rates (Fig. 6e) increased as spring continued, but dropped in the middle of the month responding to a drop in solar radiation on May 18 (see also Fig. 3). Dendrometers implied continuous stem increment growth of both trees in spring (Fig. S2c,d). Both dendrometers and soil moisture (Fig. 6 b,c) rates showed no substantial responses to the small (<5 mm) precipitation events at the end of May.

The largest precipitation event during the study period occurred on July 7 (2nd panel in Fig. 6). Soil moisture (Fig. 6b) underneath the tree canopy particularly responded to wetting after rainfall at 15 cm and 30 cm depth. The upper soil layers under the trees showed small responses and afterwards lost the water through drainage and ET, whereas the upper layer soil moisture under grassland (Fig. 6c) responded to rainfall. Dendrometers of both trees showed stem increment growth or bark swelling with the precipitation event (Fig. S2b) and shrinking for 5 days afterwards half way back to the size antecedent to precipitation. Sap flow rates of both trees (Fig. 6d, e) dropped on the day of the precipitation event.

During the period surrounding the rewetting in August and September (3rd panel in Fig. 6) dendrometers responded to the rewetting with swelling and minor shrinking during the dry days following precipitation. Sap flow (Fig. 6d,e) generally decreased for the first 3–4 days after substantial rainfall linked to decrease in VPD. PET_{norm} exceeded maple sap flow just before September rewetting started, indicating drought stress.

In the Spearmańs rank correlation analysis of daily values, precipitation characteristics, soil storage of both sites, sap flow rates, stem increment growth and LAI for both tree species were combined (Fig. 7).. Short term dynamics are not displayed in this more general overview. The regression analysis revealed a moderately (for the maple) and strong (for the birch) positive correlation between sap flow rates and LAI for both trees. LAI and stem increment growth negatively correlated for both trees likely due to opposite reactions after rainfall. Precipitation did not correlate with soil water storage, but showed moderately negative correlations with sap flow rates. Soil water storage of grassland was negatively correlated with sap flow rates and LAI, but correlated

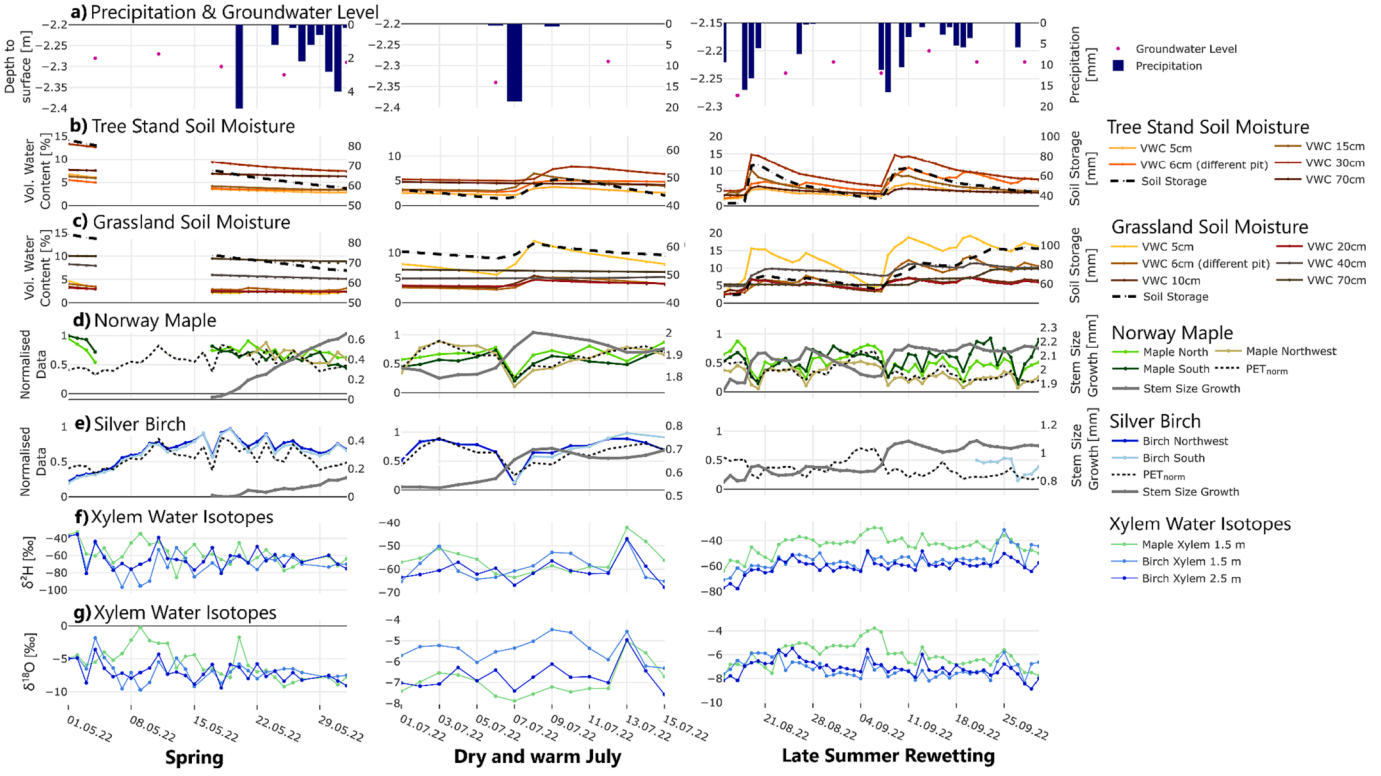

Fig. 6. Timeseries during three major time periods spring, the first half of July and the rewetting period of: daily precipitation and weekly groundwater level (a); daily soil moisture (at 5 depths) and soil storage in the first meter of the soil beneath tree canopy (b) and nearby grassland (c); daily normalised sap flow, potential evapotranspiration (PET_{norm}) and stem size growth measured for the stem-radius of the maple (d) and the birch (e); and daily median xylem water isotopes of δ^2H (f) and $\delta^{18}O$ (g).

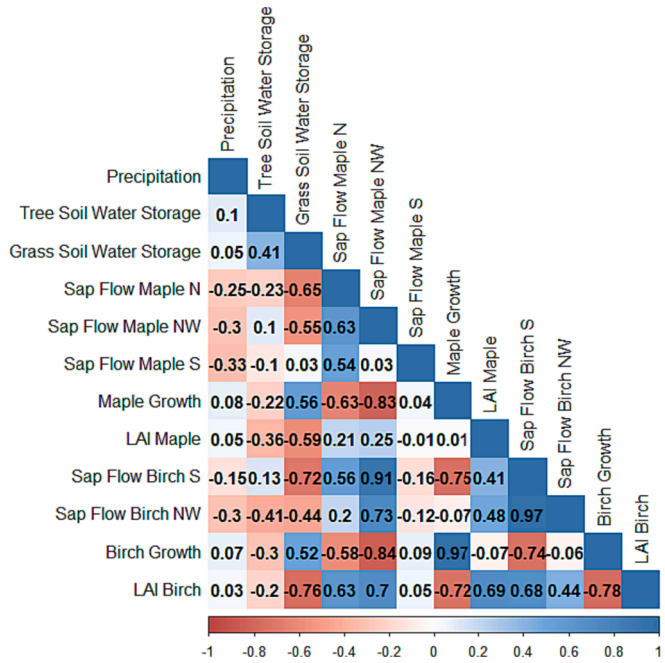

Fig. 7. Spearmańs rank correlation between daily precipitation amount [mm] and daily means of soil storage under the trees [mm], soil storage under grass [mm], sap flow of the maple north [$cm^3\ d^{-1}$], sap flow of the maple northwest [$cm^3\ d^{-1}$], sap flow of the maple south [$cm^3\ d^{-1}$], stem growth of the maple measured for the stem-radius [mm], LAI of the maple, sap flow of the birch south [$cm^3\ d^{-1}$], sap flow the birch northwest [$cm^3\ d^{-1}$], stem growth of the birch measured for the stem-radius [mm] and LAI of the birch. Numbers indicate the correlation coefficients.

positively with stem increment growth again related to reactions to precipitation.

4.3. Stable water isotope dynamics

Monitoring of δ_{xyl} was conducted from 25.04. to 20.10.2022. δ_{xyl} in both trees was enriched in heavy isotopes at the start of the study with the effect more marked in the maple tree in early May; after that all boreholes showed similar isotope signatures as spring continued (Fig. 5h,i and 6f,g). After May, the trees were depleted in heavy isotopes until the Mid of June with δ_{xyl} becoming more enriched in the 2nd half of June, being relatively constant during July and then becoming more enriched again at the time of the autumn rewetting (Fig. 5h,i and 6f,g).

Statistically, significant differences in daily median values of δ_{xyl} between tree species (Wilcoxon signed-rank test) and between borehole heights (Kruskal-Wallis test by ranks and post-hoc the pairwise Wilcoxon rank sum test with Bonferroni correction) varied depending on isotopes of δ^2H and $\delta^{18}O$ (indicating varying fractionation). Mid-summer increases of δ_{xyl} of both trees corresponded with highest LAI values (Fig. 5h,i). During rewetting in late August and September, δ_{xyl} of the maple started to deviate more from the birch and its curve strikingly resembled that of PET_{norm} (Fig. 6d,f,g). On Sep 25th δ_{xyl} of the birch borehole at 1.5 m showed quicker responses to rainfall than the 2.5 m borehole, consistent with a longer travel time of precipitation in the xylem (Fig. 6f,g).

The amount-weighted LMWL of precipitation 2022 (Fig. 8) was $\delta^2H = 7.37 \pm 0.12 * \delta^{18}O + 4.249 \pm 0.98$ ($R^2 = 0.96$) and characterised by a large range. Groundwater in comparison showed little variation, but slightly deviated from the LMWL which is likely related to the local influence and bank filtration of lake water caused by pumping at the water works. Soil water isotopes show a gradual depletion in heavy isotopes with depth. The daily timeseries of δ_{xyl} (Fig. 5h,i) and its dual isotopes (Fig. 8) showed damping and fractionated signals compared to precipitation and bulk soil water isotopes. In general, δ_{xyl} was overall

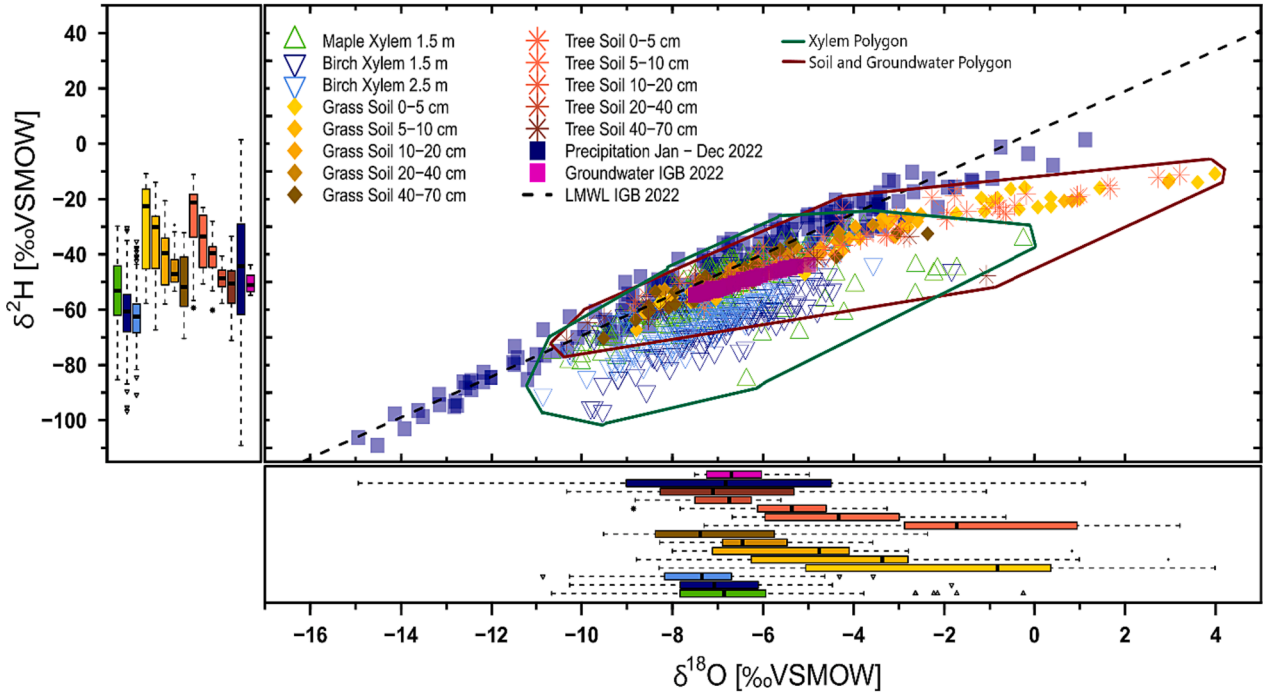

Fig. 8. Dual isotopes of daily on-site precipitation (blue squares), 2-weekly groundwater from IGB (pink squares), daily median plant xylem (δ_{xyl}) for the maple tree (one height; green triangles) and birch tree (two heights; dark/light blue upside-down triangles) and monthly bulk soil water profiles (5 depths) of the tree site underneath canopy (rhombus symbols) and of the nearby open grassland (star symbols), including polygons highlighting all δ_{xyl} signatures and soil and groundwater signatures. Data shown here were sampled between 25.04. and 20.10.2022. Boxplots show the sample distribution of the data sets. (For interpretation of the references to colour in this figure legend, the reader is referred to the web version of this article.)

much closer to the isotopic signatures of deeper soil and groundwater, likely indicating dominant sources for root water uptake. The isotopic fractionation in δ_{xyl} of both trees was apparent from the difference from source waters and the offset to the LMWL and soil water isotopes (Fig. 8). The summary statistics of the measured stable water isotopes of precipitation, groundwater, δ_{xyl} and soil water are given in Table 1. Generally, δ_{xyl} values were most similar to mean signatures of deeper soil water and groundwater.

The heat maps of bulk soil water isotopes (Fig. 9) show the development of enrichment in heavy isotopes in the upper soils compared to deeper soil signatures at both sites as summer progressed. The evaporative fractionation penetrated mostly into the first 10 cm and was highest in August and September. Moreover, grassland showed deeper penetration of enriched soil water than the tree stand at the end of the summer. The autumn depletion in heavy isotopes of the upper soils showed precipitation mixing with, and replenishing the upper soil moisture (Fig. 10).

The timeseries of daily mean stable water isotopes (Fig. 10) also shows that δ_{xyl} signatures were generally depleted in heavy isotopes and isotopically mostly like deep soil waters and groundwater (cf. Fig. 9). δ_{xyl} became more enriched in heavy isotopes in mid-summer, but depleted at the end of the dry period in August (see also Fig. 5.). $\delta^{18}O_{xyl}$ showed less evaporative fractionation effect than $\delta^{2}H_{xyl}$. δ_{xyl} lc-excess became positive towards autumn when rewetting occurred.

Table 1
Summary statistics of stable water isotopes of precipitation, groundwater, plant xylem boreholes (maple one height; birch two heights) and bulk soil water underneath tree stand and nearby grassland at upper (0.0–0.05 m) and lower depth (0.4–0.7 m) (all values in liquid phase).

	‰	min	mean	max	median	sd
Precipitation	$\delta^{2}H$	−106.28	−40.85	1.47	−37.77	21.4
	$\delta^{18}O$	−14.94	−5.9	1.12	−5.86	3.12
	lc-excess	−15.04	−1.62	11.97	−1.28	4.84
Groundwater	$\delta^{2}H$	−54.8	−50.34	−43.82	−45.93	4.00
	$\delta^{18}O$	−7.51	−6.56	−4.98	−6.95	0.85
	lc-excess	−11.37	−6.21	−3.59	−5.41	2.31
Xylem						
Maple 1.5 m	$\delta^{2}H$	−85.35	−53.33	−29.79	−53.2	11.51
	$\delta^{18}O$	−10.66	−6.83	−0.24	−6.86	1.7
	lc-excess	−42.68	−7.27	4.19	−6.215	8.8
Birch 1.5 m	$\delta^{2}H$	−96.77	−61.41	−30.5	−60.69	11.24
	$\delta^{18}O$	−10.26	−7.03	−1.84	−7.08	1.33
	lc-excess	−36.36	−13.87	6.93	−17.15	9.49
Birch 2.5 m	$\delta^{2}H$	−90.84	−62.88	−35.34	−62.46	9.25
	$\delta^{18}O$	−10.85	−7.41	−3.57	−7.35	1.21
	lc-excess	−24.52	−12.48	−0.34	−13.58	5.52
Tree Stand Soil Water						
0.0–0.05 m	$\delta^{2}H$	−53.49	−26.51	−14.12	−21.14	13.59
	$\delta^{18}O$	−6.62	−1.54	2.29	−1.59	2.95
	lc-excess	−35.27	−19.39	−8.29	−17.01	10.28
0.4 – 0.7 m	$\delta^{2}H$	−64.5	−51.68	−39.44	−54.87	8.21
	$\delta^{18}O$	−9.59	−6.84	−4.3	−7.11	1.76
	lc-excess	−17.51	−5.55	2.15	−4.8	6.96
Grassland Soil Water						
0.0–0.05 m	$\delta^{2}H$	−57.16	−28.31	−12.6	−21.98	15.39
	$\delta^{18}O$	−8.04	−1.59	3.52	−0.65	3.52
	lc-excess	−42.79	−20.81	−2.19	−17.54	11.89
0.4 – 0.7 m	$\delta^{2}H$	−62.58	−50.29	−35.2	−53.92	9.95
	$\delta^{18}O$	−8.61	−6.84	−3.26	−7.04	1.77
	lc-excess	−15.39	−4.11	1.54	−2.41	5.18

Interestingly, lc-excess of the birch showed fractionated signatures which were not corresponding with soil waters and groundwater. δ_{xyl} of both trees behaved similarly from mid of May until the rewetting in late August. Groundwater levels dropped by 0.14 m from mid-July until mid-September, but groundwater signatures were stable with deeper soil waters plotting around it. Precipitation signatures showed summer enrichment in heavy isotopes in occasional summer rainfall with small magnitude and depletion in September (Fig. 10).

To get a clearer picture of seasonal and drought dynamics, we again "zoomed" into three time periods in more detail(Fig. 11: spring (a), the first half of July (b) and the rewetting period (c)). Fig. 11 (a) shows the start of the *in-situ* xylem measurements during leaf out in May. Here, δ_{xyl} signatures of both species varied during the first half of the month and started to show more similar patterns at the end of the month when frequent precipitation events occurred. For both trees, δ_{xyl} resembled that of deeper soil waters, whereas upper soils showed mixing with precipitation. During the dry and hot period in July with the largest rainfall event (18 mm, Fig. 11 b), δ_{xyl} signatures moved in the direction of precipitation signals, but also showed signals of groundwater isotopes. Lc-excess of δ_{xyl} of the birch was lower than of the maple indicating higher fractionation during drought. The rewetting period in August and September (Fig. 11 c) revealed that δ_{xyl} was again most similar to signatures of deeper soil waters and groundwater. Also, δ_{xyl} and deep soil picked up most of the precipitation signals during rewetting. Lc-excess of xylem increased towards autumn/leaf senescence. Finally, precipitation signals showed autumn depletion in heavy isotopes.

5. Discussion

5.1. Seasonality and drought effects in ecohydrological fluxes and water cycling of urban trees

By combining the monitoring of stable water isotopes with sap flow, stem size growth, LAI, midday twig water potential, soil moisture measurements and climate data, we gained novel insights into water cycling of non-irrigated urban trees during the full growing period 2022 (April-November). Our study also included a marked drought in the summer of 2022. Thus, we were able to monitor the daily ecohydrological fluxes in trees in an urban green space under hot and dry conditions (summarising conceptual graphic: Fig. 12), which can be a threat to city trees (Marchin et al., 2022).

Ecohydrological dynamics in the trees showed their most substantial range at the beginning of the growing period with regular precipitation inputs after spring leaf out: The largest increase of both trees' LAI and stem increments together with the largest alterations of δ_{xyl} was observed in May and June, while soil moisture was decreasing especially underneath the tree canopy. Generally, the stem size growth of both trees was positively correlated with precipitation, which could partly reflect swelling that does not necessarily contribute to growth (Szymczak et al., 2020). Previous studies detected swelling during rainfall and shrinking in the 3 days after precipitation as we did in our dendrometer data (Chan et al., 2016; Herrmann et al., 2016). δ_{xyl} signatures in both trees were depleted at the start of the study in May, with the effect more marked in the maple. This suggests a dependence of δ_{xyl} on species-specific storage effects over the winter and a distinct start of transpiration signals (Améglio et al., 2002; Hao et al., 2013; Sánchez-Costa et al., 2015).

At the beginning of July, mid-summer enrichment of δ_{xyl} was observed, which matches the findings of a recent study of trees in the parks of Berlin by Marx et al., (2022). From early July until mid-August precipitation events were low in frequency and magnitude (mostly all below 5 mm) and combined with high temperatures. Our *in-situ* monitoring of δ_{xyl} during the summer drought indicated that deeper sources of soil water and groundwater sustained both trees. The distinct isotopic signal of the upper soil water, which was enriched in heavy isotopes, was

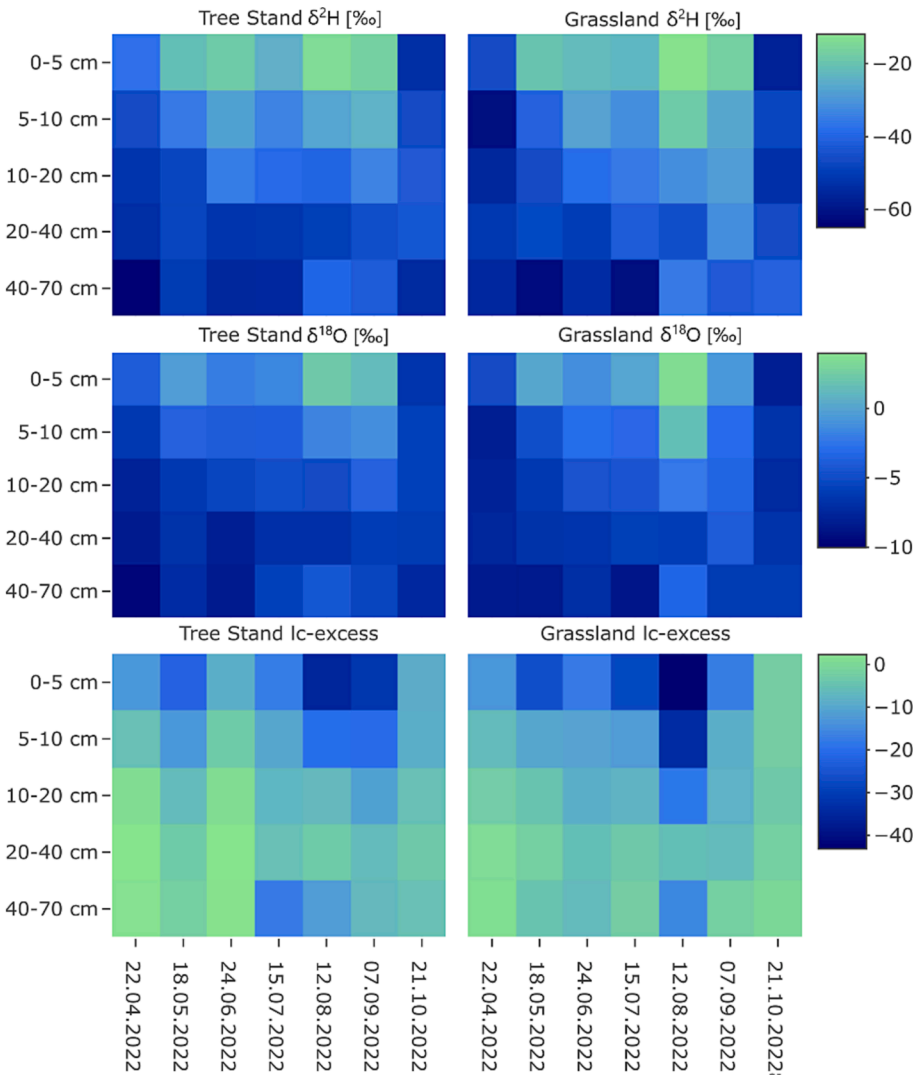

Fig. 9. Heat maps of bulk soil water isotopes from monthly destructive sampling at the tree stand and the grassland site.

not reflected in δ_{xyl}. Such uptake of deep water sources in δ_{xyl} has been observed as a common strategy of trees during dry conditions (Ellsworth & Sternberg, 2014; Kühnhammer et al., 2023).

We only detected a stronger precipitation signal in δ_{xyl} after the only major precipitation event (>18 mm), but signals of other summer precipitation events, which were all < 5 mm, were not evident in δ_{xyl}. This is consistent with the work of Kühnhammer et al. (2022) and Landgraf et al. (2022) who also observed no response of δ_{xyl} to single precipitation events. Other recent studies saw fractionation as evaporative enrichment of δ_{xyl} occurring during dry spells when transpiration is limited (Martín-Gómez et al., 2016; Barbeta et al., 2020; Beyer et al., 2020). However, in our study, δ_{xyl} was depleted in heavy isotopes compared to source waters; which might point towards a contribution of biogeochemical processes and organics to fractionation (see discussion on fractionation in 5.2). These internal processes preclude apportionment of root water uptake by simple mixing models and need to be incorporated in process-based models that capture internal routing and mixing of soil water within the tree (cf. Smith et al., 2022).

In our ecohydrological monitoring we saw various tree responses to the dry spell. Both trees showed slight shrinking and no stem increment growth during that period, which can be explained through a tree water deficit-induced shrinking of the stem that causes imbalances between transpiration and root water uptake (Zweifel et al., 2005), e.g. stored trunk water being used to sustain the transpiration stream. A recent study on urban Scot pines also reported that summer drought intensifies stem shrinking and reduces annual tree growth (Rocha & Holzkämper, 2023). Similar to our study, their highest stem size growth rates occurred in May and June and stagnated as of the summer drought in July. Occasional cessation of stem size growth during dry conditions was also reported for Mediterranean *Quercus ilex* (Gutiérrez et al., 2011) and in a tropical dry forest (García-Cervigón et al., 2017). However, during conditions of ample water supply, growth rates of poplar trees started stagnating only in late August (McLaughlin et al., 2003).

In August, we detected a drop in LAI. Such a decline in LAI after extended heat and drought was previously reported in remote sensing studies (Liu et al., 2012; Mendes de Moura et al., 2015). During that time, the sandy soils at the study site were extremely dry. The low soil storage capacity and soil moisture deficit had negative impacts on vegetation productivity (Conradt et al., 2023): E.g., the more negative midday water potential in July and August in conjunction with observed tree shrinkage, suggest that the investigated urban trees relied on internal water storage as a compensation strategy under drought (Preisler et al., 2022), under reduced soil moisture and lower groundwater levels. P50 values, e.g. the water potential at 50 % loss of conductance, are a useful indicator for plant water stress, but they vary strongly in the literature for the two tree species. For example, Lu et al. (2022) describe P50 of Maple to range from 0.5 to 1.7 MPa and of Birch from −1.5 to −2.2 MPa based on hydraulic modelling. Water potential observed in

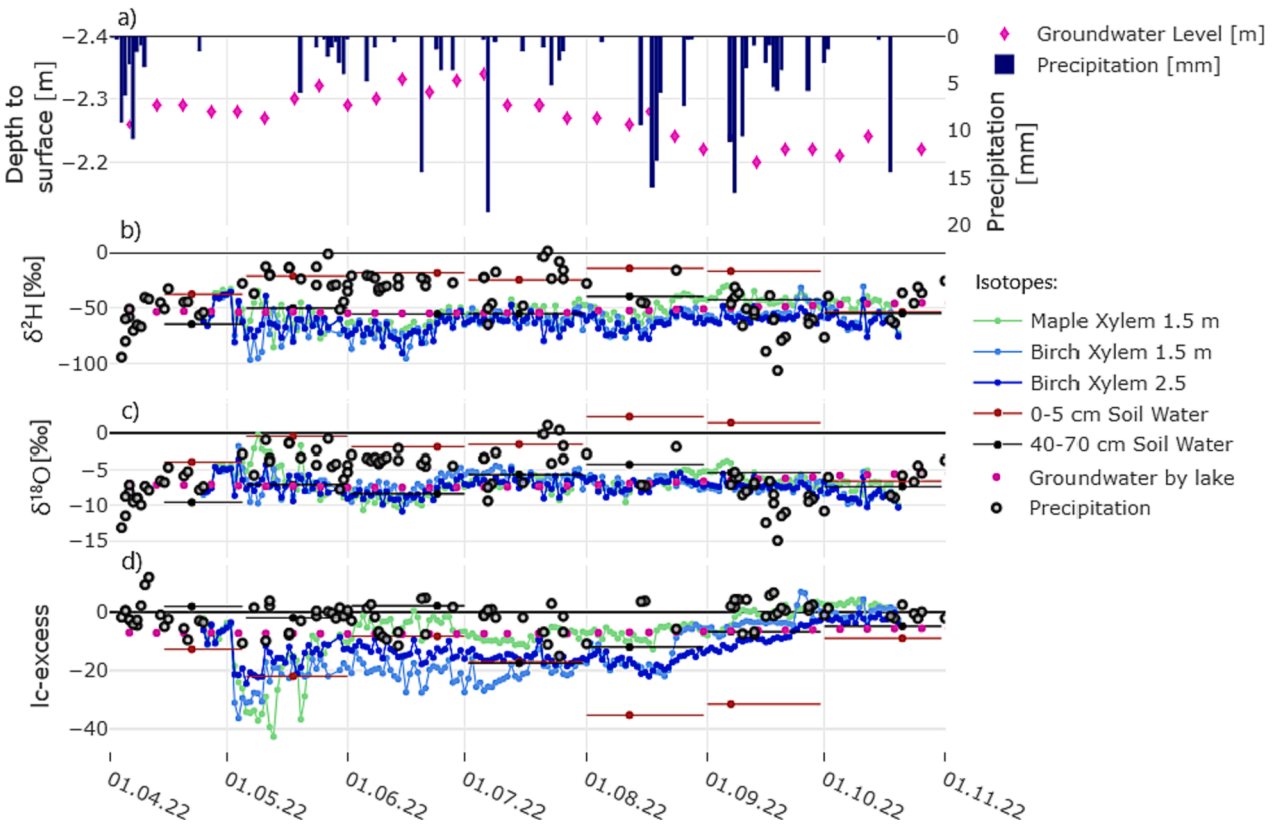

Fig. 10. Daily precipitation and weekly groundwater level (a) and full period of daily median stable water isotopes of tree xylem (one height for maple, 2 heights for birch tree), bulk soil water at the tree stand, groundwater and precipitation in (b) δ^2H, (c) $\delta^{18}O$ and (d) lc-excess.

this study did not exceed −1.5 MPa. Consequently, the responses of the observed trees to drought – use of deeper soil water sources, stem shrinking – appear to prevent severe water/drought stress and reductions in physiological activity.

Interestingly, sap flow rates did not show major reductions in the trees during the drought period. PET_{norm} (index for atmospheric demand, cf. Bliss Singer et al., 2021) exceeded $sapflow_{norm}$ only for a few days in early August and early September, but not consistently. This suggests that the trees were resilient to the drought and the rooting zone did not dry sufficiently to cause the trees to limit transpiration losses. Moreover, the decline in LAI probably lowered the water demand during that period. Normal tree transpiration was generally sustained throughout the study period, e.g. by internal water storage or deeper water supply contributing to transpiration also when stem size indicated shrinking. A reason for the low drought stress or even lack of it (seen in the sap flow rates) could be the type of trees investigated. Previous studies showed that *Acer platanoides* have high drought tolerance in cities (Kunz et al., 2016) and maples tended to use a deep water source under high vapor pressure deficit even when shallow soil water was available (Lanning et al., 2020). However, the genus *Acer* has shown significant stem increment growth decline in drought years (Gillner et al., 2014) and street maples have shown low leaf gas exchange rates indicating non-economical water consumption (Gillner, Korn & Roloff, 2015). *Betula pendula*, which is less common than maple in German cities, is often associated with freesly draining soils and has been shown to maintain high sap flow rates and high water use efficiencies even during drought in forests (Baumgarten et al., 2019).

During the rewetting in late August and September, soil moisture slightly increased, but most of the water percolated rapidly after rainfall due to the sandy soil which has very poor water retention properties. These soil characteristics are a general constraint on vegetation productivity in the Berlin-Brandenburg region during extended droughts (Drastig et al., 2011). Still, the measured ψ responded to precipitation inputs with increased values, revealing improved water availability for the maple and birch.

Finally, the drought response of the two trees was visible in the use of deep water sources, the restrained stem increment growth, lowered LAI and ψ, but stable sap flow rates were sustained by deeper water sources and deeper roots. Therefore, urban trees and shrubs with shallow root development are likely to be more vulnerable to dry summers (cf. Gessler et al. (2022)) posing a particular threat in future accelerated summer droughts combined with insufficient autumn rewetting causing water content to also drop in deeper soils.

5.2. *Value of continuous, in-situ monitoring of xylem water isotopes to understand sources of urban tree water uptake*

Here, we investigated the SPAC of an urban critical zone to understand urban tree water cycling. By combining high resolution *in-situ* monitoring of δ_{xyl} with stable water isotopes of daily precipitation, weekly groundwater and monthly soil water at different depths, we gathered valuable insights on the ecohydrology of urban tree stands.

Stable water isotopes of precipitation showed summer enrichment and autumn depletion in heavy isotopes, which was also observed for Berlin by Kuhlemann et al. (2021) and is globally driven by the dominance of temperature and precipitation amount (Bowen, 2008). Groundwater isotopes showed some fractionation by slightly deviating from the LMWL, which likely is an influence from the nearby lake and pumping of lake water by the water works (cf. Landgraf et al., 2022). The monthly bulk sampling of soil water for isotope analysis at different depths complemented the *in-situ* monitoring of δ_{xyl} revealing the potential sources of root uptake.

Importantly, our δ_{xyl} dataset showed that *in-situ* borehole measurements are reliable over long periods (179 d) in urban environments

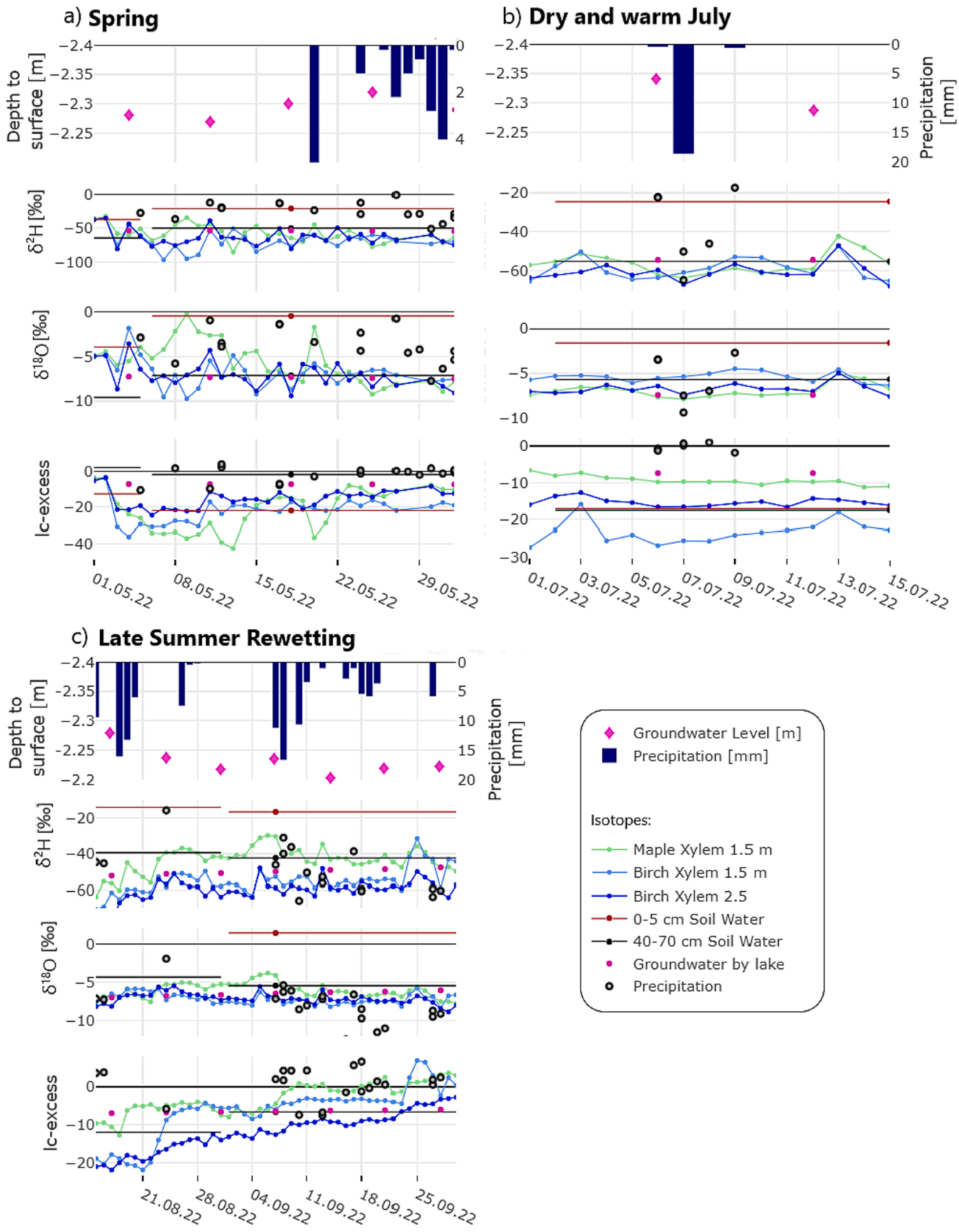

Fig. 11. Timeseries during three important selected time periods spring (a), the first half of July (b) and the rewetting period (c) of: daily precipitation and weekly groundwater levels and daily median stable water isotopes of tree xylem (one height for maple, 2 heights for birch tree), bulk soil water at the tree stand (2 depths: upper soil 0–5 cm and deeper soil 40–70 cm), groundwater and precipitation in δ^2H, $\delta^{18}O$ and lc-excess.

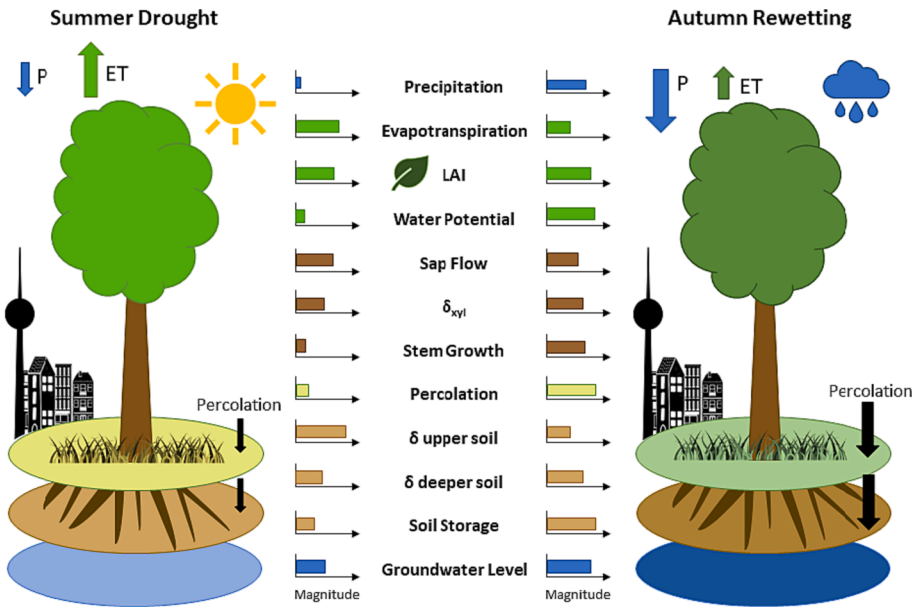

Fig. 12. Conceptual graphic summarising the main ecohydrological fluxes observed at urban trees during the summer drought (July until Mid-August) and under rewetting conditions (Mid-August until September) in 2022. Lighter colours mean drier conditions, darker colors mean moister conditions.

under non-laboratory conditions, capturing inherent variability within the stem, if condensation and wounding issues are controlled. This confirms several recent studies that successfully applied *in-situ* monitoring to detect the underlying processes of tree water cycling (Volkmann et al., 2016; Mennekes et al., 2021; Seeger & Weiler, 2021; Kühnhammer et al., 2022; Landgraf et al., 2022). Most importantly, we could identify the predominant sources of tree water uptake of two tree species in an urban green space: δ_{xyl} signatures were closest to deep soil water and possibly groundwater which implies the use of deeper sources due to deep tree roots tapping into older water in combination with the absence of available moisture in urban surface horizons (cf. Bijoor et al., 2011; Gómez-Navarro et al., 2019). This is also consistent with previous studies in Berlin's green spaces of Marx et al. (2022), where *Acer platanoides* increasingly used deeper sources from spring until end of August and with the work of Kuhlemann et al., (2021), who observed signals for deep root water uptake from larger trees. Interestingly, during rewetting conditions, a distinct travel time in the xylem at different stem heights could be detected for the birch boreholes after the rain event on Sep 25. The precipitation signal took one day to travel from 1.5 m to 2.5 m height in the tree.

The δ_{xyl} was fractionated plotting below and somewhat parallel to the LMWL in the dual isotope plot (Benettin et al., 2021). Such fractionation of δ_{xyl} needs to be considered when studying the likely sources of tree water uptake. Xylem isotopes can be fractionated since only fractions of precipitation inputs are taken up by trees (Allen et al., 2022). Fractionation of δ_{xyl} has often been attributed to cryogenic extraction effects (e.g. Chen et al., 2020; Snelgrove et al., 2021; Wen et al., 2022), which can be ruled out in our *in-situ* study. Other explanations might be biogeochemical processes or organic interference in the sample (Nehemy et al., 2019; von Freyberg et al., 2020), µm-scale heterogeneity in the isotope ratios of water within woody stems and soil micro-pores (Barbeta et al., 2022), the general tree root morphology and related preferences that cause general fractionation at tree root (Ellsworth & Sternberg, 2014), as well as evaporation through the tree bark (Dawson & Ehleringer, 1991; Smith et al., 1997). Vega-Grau et al. (2021) also report a general fractionation along the transpiration path of a trees xylem stream: They argue that δ_{xyl} fractionation is possibly caused by both below- and aboveground processes like individual roots not picking up soil water or using different proportions of the water source (root-soil offsets), which may further vary by species root morphologies. Additionally, Kühnhammer et al. (2023) observed that the amount of water uptake can be low during drought because of reduced sap flow, which could be another reason for fractionation of δ_{xyl}.

Further, tree stems naturally transport and produce CH_4 (Covey & Megonigal, 2018). Biogenic CH_4 could have influenced the hydrogen isotope composition measured in the boreholes as it is travelling in the sap with the stem water (Anttila et al., 2024). This is a possible explanation for the fractionated δ_{xyl} signals at least for the maple in our study: During δ_{xyl} measurements high CH_4 signals were detected in both maple boreholes and in the birch borehole at 1.5 m height during the start of each measurement. Those signals were higher than the usual tropospheric CH_4 concentrations in the CRDS. To our knowledge, CH_4 signals have rarely been reported or discussed as reasons for fractionated signals using *in-situ* borehole method. Only Zhao et al. (2016) investigated a possible relation of CH_4 to xylem fractionation in the cryogenic vacuum distillation method. They compared the original xylem sap of *Populus euphratica Oliv.* with xylem sap distillate and found no difference.

We conclude that potential reasons for fractionation shown as plant-source offset in our δ_{xyl} data include a combination of heterogenous water uptake strategies, internal routing, mixing and physiological processes (similar to Snelgrove et al., 2021). In particular, δ_{xyl} of birch was more fractionated, which could be due to its location near a building. Possibly, urban infrastructure leads to δ_{xyl} fractionation by influencing the trees root morphology. Importantly, if the potential reasons for fractionation in δ_{xyl} are identified (Barbeta et al., 2019) and the fractionation signals are small compared to the genuine isotopic signals of the data (Allen & Kirchner, 2022), datasets containing fractionated δ_{xyl} are beneficial to understanding plant water sources (Benettin et al., 2021; Landgraf et al., 2022).

5.3. Wider implications

Urban trees play a significant role for climate resilient cities (Peng et al., 2012; Siehr et al., 2022), but accelerating droughts make them vulnerable and may cause loss of their climate benefits (Burley et al., 2019). Understanding the water cycling in non-irrigated urban trees under drought conditions and also about the potential differences in the resilience of different species provides the basis for designing sustainable management of urban green spaces with focus on plant water supply. However, urban ecosystems and their water partitioning are

highly complex, as green spaces are heterogenous in type and size, different species, water supply is highly varying, water flow patterns are modified and soils are altered (Gessner et al., 2014).

The current literature on urban tree water cycling mostly consists of studies combining remote sensing data and modelling (Litvak et al., 2017; Vulova et al., 2023) or non-continuous ecohydrological monitoring (Bijoor et al., 2011) only depicting excerpts during a year. High-resolution *in-situ* monitoring of urban tree δ_{xyl} helps to reveal the complex processes in urban trees at the plot-scale -particularly if monitored over entire vegetative periods – provides detailed insights on urban tree water cycling (Landgraf et al., 2022), which are needed to improve urban planning. However, *in-situ* studies on urban trees using stable water isotopes of plants are very rare. As our study was carried out in an extreme dry summer, it also provides a first assessment on how non-irrigated mature urban trees react to changing water supply throughout the full vegetative period.

Even if based on only two tree species and trees, our results clearly suggest a dependence on deep water sources of these deciduous urban trees, which has several implications for urban tree management: At open tree stands in parks that are interacting with adjacent grasslands, adequate natural water supply needs to be ensured and (sub)surface flow patterns understood (Kuhlemann et al., 2021). Further, the seasonal variability in changes in root water sources need to be considered. Street trees are especially vulnerable to droughts because their root space is often limited and soils are not connected (Czaja et al., 2020). If the focus of this study would have been on street trees or trees in highly developed areas these trees would likely have shown lower sap flow rates due to even drier conditions and water would be most likely mainly sourced from upper soils as irrigation would be the substantial water source. This underlines the need for choosing sustainable site-adapted tree cell applications for street trees with right planning of root barriers for appropriate root space (Pauleit, 2003). Also the influence of leaking pipes and road or pavement runoff in more developed urban areas should not be neglected, which can provide sufficient water amounts for city trees. In addition, urban green space planning for drought requires climate resilient species (Marchin et al., 2022) that fit into varying city landscapes. For this, the water use strategies and cooling potentials of individual trees and also groups of the different tree species needs to be considered (Gillner & Vogt et al., 2015; Gillner et al., 2017; Marx et al., 2022).

Despite the knowledge on the likely water sources of the monitored trees, our results also gave first insights on the temporal dynamics of urban tree water storage patterns of Norway maple and silver birch throughout the growing period, which is important as stored water can be as much as 20 % of transpiration sustaining xylem transport (Cermák et al., 2007). In some cases, natural replenishment from precipitation will not be sufficient for urban green spaces while in the meantime, urban water reserves are often too scarce to irrigate trees extensively. A solution would be to use rainwater from high-magnitude precipitation events which are becoming more frequent (Hodnebrog et al., 2019; Myhre et al., 2019) by improving flowpaths and storing precipitation via rainwater harvesting (Suleiman et al., 2020), e.g. from roof runoff (Papasozomenou et al., 2019; Gillefalk et al., 2021; Gillefalk et al., 2022).

We are confident that our approach and results are transferable to other urban areas across the globe that are suffering from increasing periods of drought and heat. But as all cities have their own very heterogenous infrastructure and surfaces, all management decisions need to be made individually (Nowak & Dwyer, 2007). Still, our findings are relevant for various deciduous tree species and regions that match the environmental requirements of the respective latitude and climate. Eventually, there is always a nexus between planning urban green spaces as functioning ecosystem and improving its catchment hydrology (Livesley et al., 2016).

We see strong potential for future studies that investigate the sub-daily dynamics of urban tree water cycling via *in-situ* monitoring of δ_{xyl}, e.g. for revealing species specific travel times between different heights (cf. Seeger and Weiler (2021)) or to reveal diurnal drought responses between varying types of urban green spaces (e.g. sizes, species, type of use). Also, a comparison of different years varying between dry and wet extremes would further increase insights on urban tree water cycling in varying climate extremes. Future modelling work will integrate our field-based data into a process-based model (cf. Smith et al. (2022); Gillefalk et al. (2021)), for short- and long-term assessment of water availability for plant growth. This will lead to a more complete picture of urban tree water cycling improving future related research.

6. Conclusion

We monitored stable water isotopes in the xylem (δ_{xyl}) of a maple and a birch tree using *in-situ* cavity ring-down spectroscopy (CRDS) over the full vegetative period of 2022 in an urban green space area in Berlin, Germany. By integrating this with monitoring of vegetation dynamics via sap flow, stem increments, LAI, groundwater levels and soil moisture measurements at different depths, we gained novel insights on the water cycling of non-irrigated urban trees.

The monitoring period was characterised by a spring with average precipitation inputs, followed by an extremely dry period from July until mid-August and a constant rewetting from the end of August until October. Our unique (for urban settings) integrated dataset revealed highest changes in the ecohydrological dynamics of the investigated maple and birch tree at the beginning of the growing period with increases in stem size and LAI, but also decreasing soil moisture. During summer, drought stress was apparent in the ecohydrological fluxes of the monitored trees in the reduction of stem increment growth, LAI, midday water potential and soil moisture. Yet sap flow rates were overall stable and tree transpiration was preserved. The measured δ_{xyl} signatures were isotopically in the range of deep soil waters and groundwater implying that deeper sources were mainly sustaining the trees water supply during the drought. We also detected fractionation of δ_{xyl}, which is possibly induced by heterogenous water uptake strategies and biochemical processes in the tree xylem, including CH_4 transport.

Our results suggest that urban trees rely on deep water supply and internal storage during drought. We hypothesise that urban trees and shrubs with shallow root development will be more vulnerable to dry summers, and we see a special threat in future accelerated summer droughts combined with insufficient autumn rewetting causing deep soil layers to dry out. Our findings have critical implications for urban isotope-based ecohydrological and catchments studies that are integrated into process-based models. Urban green space planning and water management can benefit from our study towards urban trees being more resilient to accelerating droughts.

CRediT authorship contribution statement

A-M. Ring: Data curation, Writing – original draft, Visualization, Investigation, Validation, Formal analysis, Methodology. **D. Tetzlaff:** Conceptualization, Funding acquisition, Writing – review & editing, Validation, Supervision, Resources, Project administration, Software. **M. Dubbert:** Writing – review & editing, Investigation, Methodology. **J. Freymueller:** Data curation, Investigation, Methodology. **C. Soulsby:** Conceptualization, Writing – review & editing, Validation, Supervision.

Declaration of competing interest

The authors declare the following financial interests/personal relationships which may be considered as potential competing interests: Doerthe Tetzlaff reports financial support, administrative support, and equipment, drugs, or supplies were provided by German Research Foundation.

Data availability

Data will be made available on request.

Acknowledgements

This study was funded through the German Research Foundation (DFG) as part of the Research Training Group "Urban Water Interfaces" (UWI; GRK2032/2) and the Einstein Foundation as part of the "Modelling surface and groundwater with isotopes in urban catchments" (MOSAIC) project. Funding for DT was also received through the Einstein Research Unit "Climate and Water under Change" from the Einstein Foundation Berlin and Berlin University Alliance (grant no. ERU-2020-609) and the project BiNatur (BMBF No. 16LW0156). We also acknowledge the BMBF (funding code 033W034A), which supported the stable isotope laboratory and in-situ laser analyser. Contributions from CS have also been supported by the Leverhulme Trust through the ISO-LAND project (grant no. RPG 2018 375). We thank all colleagues involved in the daily precipitation, groundwater sampling, sensor installations and soil water isotope sampling, in particular Jan Christopher, Hauke Dämpfling, Lisa Grof, Jessica Landgraf, Grit Siegert and Johanna Stralendorff.

Appendix A. Supplementary data

Supplementary data to this article can be found online at https://doi.org/10.1016/j.jhydrol.2024.131020.

References

Aboelnga, H., Ribbe, L., Frechen, F.-B., Saghir, J., 2019. Urban water security: definition and assessment framework. Resources 8 (4), 178. https://doi.org/10.3390/resources8040178.

Allen, R.G., 1998. Crop evapotranspiration-guideline for computing crop water requirements. Irrigation and Drain 56, 300. https://ci.nii.ac.jp/naid/10015358529/.

Allen, S.T., Kirchner, J.W., 2022. Potential effects of cryogenic extraction biases on plant water source partitioning inferred from xylem-water isotope ratios. Hydrol. Process. 36 (2) https://doi.org/10.1002/hyp.14483.

Allen, S.T., Sprenger, M., Bowen, G.J., Brooks, J.R., 2022. Stable isotopes in tree rings: spatial and temporal variations in plant source water: O and H isotope ratios from precipitation to xylem water. In: Siegwolf, R.T.W., Brooks, J.R., Roden, J., Saurer, M. (Eds.), Stable Isotopes in Tree Rings: Spatial and Temporal Variations in Plant Source Water: O and H Isotope Ratios from Precipitation to Xylem Water. Springer International Publishing, Cham, pp. 501–535.

Améglio, T., Bodet, C., Lacointe, A., Cochard, H., 2002. Winter embolism, mechanisms of xylem hydraulic conductivity recovery and springtime growth patterns in walnut and peach trees. Tree Physiol. 22 (17), 1211–1220. https://doi.org/10.1093/treephys/22.17.1211.

Amt für Statistik Berlin-Brandenburg *Bevölkerungsstand 2022*. https://www.statistik-berlin-brandenburg.de/bevoelkerung/demografie/bevoelkerungsstand [Accessed 30 March 2023].

Anttila, J., Tikkasalo, O.-P., Hölttä, T., Lintunen, A., Vainio, E., Leppä, K., et al., 2024. Model of methane transport in tree stems: case study of sap flow and radial diffusion. Plant Cell Environ. 47 (1), 140–155. https://doi.org/10.1111/pce.14718.

Arnfield, A.J., 2003. Two decades of urban climate research: a review of turbulence, exchanges of energy and water, and the urban heat island. Int. J. Climatol. 23 (1), 1–26. https://doi.org/10.1002/joc.859.

Barbeta, A., Jones, S.P., Clavé, L., Wingate, L., Gimeno, T.E., Fréjaville, B., et al., 2019. Unexplained hydrogen isotope offsets complicate the identification and quantification of tree water sources in a riparian forest. Hydrol. Earth Syst. Sci. 23 (4), 2129–2146. https://doi.org/10.5194/hess-23-2129-2019.

Barbeta, A., Gimeno, T.E., Clavé, L., Fréjaville, B., Jones, S.P., Delvigne, C., et al., 2020. An explanation for the isotopic offset between soil and stem water in a temperate tree species. New Phytol. 227 (3), 766–779. https://doi.org/10.1111/nph.16564.

Barbeta, A., Burlett, R., Martín-Gómez, P., Fréjaville, B., Devert, N., Wingate, L., et al., 2022. Evidence for distinct isotopic compositions of sap and tissue water in tree stems: consequences for plant water source identification. New Phytol. 233 (3), 1121–1132. https://doi.org/10.1111/nph.17857.

Bastin, J.-F., Clark, E., Elliott, T., Hart, S., van den Hoogen, J., Hordijk, I., et al., 2019. Correction: understanding climate change from a global analysis of city analogues. PLoS One 14 (10), e0224120.

Bastos, A., Orth, R., Reichstein, M., Ciais, P., Viovy, N., Zaehle, S., et al., 2021. Vulnerability of european ecosystems to two compound dry and hot summers in 2018 and 2019. Earth Syst. Dyn. 12 (4), 1015–1035. https://doi.org/10.5194/esd-12-1015-2021.

Baumgarten, M., Hesse, b.d., augustaitienė, i., marozas, v., mozgeris, g. & byčenkienė, s., et al., 2019. Responses of species-specific sap flux, transpiration and water use efficiency of pine, spruce and birch trees to temporarily moderate dry periods in mixed forests at a dry and wet forest site in the hemi-boreal zone. J. Agric. Meteorol. 75 (1), 13–29. https://doi.org/10.2480/agrmet.D-18-00008.

Benettin, P., Nehemy, M.F., Cernusak, L.A., Kahmen, A., McDonnell, J.J., 2021. On the use of leaf water to determine plant water source: a proof of concept. Hydrol. Process. 35 (3) https://doi.org/10.1002/hyp.14073.

Beyer, M., Kühnhammer, K., Dubbert, M., 2020. In situ measurements of soil and plant water isotopes: a review of approaches, practical considerations and a vision for the future. Hydrol. Earth Syst. Sci. 24 (9), 4413–4440. https://doi.org/10.5194/hess-24-4413-2020.

Bichai, F., Cabrera Flamini, A., 2018. The water-Sensitive City: implications of an urban water management paradigm and its globalization. WIREs. Water 5 (3). https://doi.org/10.1002/wat2.1276.

Bijoor, N.S., McCarthy, H.R., Zhang, D., Pataki, D.E., 2011. Water sources of urban trees in the Los Angeles metropolitan area. Urban Ecosystems 15 (1), 195–214. https://doi.org/10.1007/s11252-011-0196-1.

Bliss Singer, M., Asfaw, D.T., Rosolem, R., Cuthbert, M.O., Miralles, D.G., MacLeod, D., et al., 2021. Hourly potential evapotranspiration at 0.1° resolution for the global land surface from 1981-present. Sci. Data 8 (1), 224. https://doi.org/10.1038/s41597-021-01003-9.

Bolund, P., Hunhammar, S., 1999. Ecosystem services in urban areas. Ecol. Econ. 29 (2), 293–301. https://doi.org/10.1016/S0921-8009(99)00013-0.

Bonferroni, C.E., 1935. Il calcolo delle assicurazioni su gruppi di teste. Studi in Onore Del Professore Salvatore Ortu Carboni 13–60.

Bowen, G.J., 2008. Spatial analysis of the intra-annual variation of precipitation isotope ratios and its climatological corollaries. J. Geophys. Res. Atmos. 113 (D5), n/a-n/a. https://doi.org/10.1029/2007JD009295.

Burley, H., Beaumont, L.J., Ossola, A., Baumgartner, J.B., Gallagher, R., Laffan, S., et al., 2019. Substantial declines in urban tree habitat predicted under climate change. Sci. Total Environ. 685, 451–462. https://doi.org/10.1016/j.scitotenv.2019.05.287.

Cermák, J., Kucera, J., Bauerle, W.L., Phillips, N., Hinckley, T.M., 2007. Tree water storage and its diurnal dynamics related to sap flow and changes in stem volume in old-growth Douglas-fir trees. Tree Physiol. 27 (2), 181–198. https://doi.org/10.1093/treephys/27.2.181.

Chan, T., Hölttä, T., Berninger, F., Mäkinen, H., Nöjd, P., Mencuccini, M., et al., 2016. Separating water-potential induced swelling and shrinking from measured radial stem variations reveals a cambial growth and osmotic concentration signal. Plant Cell Environ. 39 (2), 233–244. https://doi.org/10.1111/pce.12541.

Chen, Y., Helliker, B.R., Tang, X., Li, F., Zhou, Y., Song, X., 2020. Stem water cryogenic extraction biases estimation in deuterium isotope composition of plant source water. PNAS 117 (52), 33345–33350. https://doi.org/10.1073/pnas.2014422117.

Conradt, T., Engelhardt, H., Menz, C., Vicente-Serrano, S.M., Farizo, B.A., Peña-Angulo, D., et al., 2023. Cross-sectoral impacts of the 2018–2019 central european drought and climate resilience in the german part of the Elbe River basin. Reg. Environ. Chang. 23 (1), 32. https://doi.org/10.1007/s10113-023-02032-3.

Covey, K.R., Megonigal, J.P., 2018. Methane production and emissions in trees and forests. New Phytol. 222 (1), 35–51. https://doi.org/10.1111/nph.15624.

Czaja, M., Kołton, A., Muras, P., 2020. The complex issue of urban trees—Stress factor accumulation and ecological service possibilities. Forests 11 (9), 932. https://doi.org/10.3390/f11090932.

Dawson, T.E., Ehleringer, J.R., 1991. Streamside trees that do not use stream water. Nature 350 (6316), 335–337. https://doi.org/10.1038/350335a0.

de Deurwaerder, H.P.T., Visser, M.D., Detto, M., Boeckx, P., Meunier, F., Kuehnhammer, K., et al., 2020. Causes and consequences of pronounced variation in the isotope composition of plant xylem water. Biogeosciences 17 (19), 4853–4870. https://doi.org/10.5194/bg-17-4853-2020.

Dodman, D., Hayward, B., Pelling, M., Castan Broto, V., Chow, W., Chu, E., Ipcc, et al., 2023. Cities, settlements and key infrastructure. In: Climate Change 2022 – Impacts, Adaptation and Vulnerability. Cambridge University Press, pp. 907–1040.

Drastig, K., Prochnow, A., Baumecker, M., Berg, W. & Brunsch, R. (2011) Agricultural Water Management in Brandenburg. *DIE ERDE – Journal of the Geographical Society of Berlin,* 2011, pp. 119–140. https://www.die-erde.org/index.php/die-erde/article/view/45 [Accessed 10 August 2023].

Duarte Rocha, A., Vulova, S., Meier, F., Förster, M., Kleinschmit, B., 2022. Mapping evapotranspirative and radiative cooling services in an urban environment. Sustain. Cities Soc. 85, 104051 https://doi.org/10.1016/j.scs.2022.104051.

Dubbert, M., Werner, C., 2018. Water fluxes mediated by vegetation: emerging isotopic insights at the soil and atmosphere interfaces. New Phytol. 221 (4), 1754–1763. https://doi.org/10.1111/nph.15547.

Dwd, 2023a. Climate data center (CDC) of german weather service. Accessed 10 April 2023. https://opendata.dwd.de/climate_environment/CDC/observations_germany/climate/daily/kl/.

Dwd, 2023b. Longterm means. Accessed 3 July 2023. https://www.dwd.de/DE/leistungen/klimadatendeutschland/vielj_mittelwerte.html.

Dwyer, J.F., Schroeder, H.W. & Gobster, P.H. (1991) The significance of urban trees and forests: toward a deeper understanding of values, 276–284.

Ehleringer, J.R., Barnette, J.E., Jameel, Y., Tipple, B.J., Bowen, G.J., 2016. Urban water - a new frontier in isotope hydrology. Isot. Environ. Health Stud. 52 (4–5), 477–486. https://doi.org/10.1080/10256016.2016.1171217.

Ellsworth, P.Z., Sternberg, L.S.L., 2014. Seasonal water use by deciduous and evergreen woody species in a scrub community is based on water availability and root distribution. Ecohydrology 8 (4), 538–551. https://doi.org/10.1002/eco.1523.

Fabiani, G., Schoppach, R., Penna, D., Klaus, J., 2022. Transpiration patterns and water use strategies of beech and oak trees along a hillslope. Ecohydrology 15 (2). https://doi.org/10.1002/eco.2382.

García-Cervigón, A.I., Camarero, J.J., Espinosa, C.I., 2017. Intra-annual stem increment patterns and climatic responses in five tree species from an ecuadorian tropical dry forest. Trees 31 (3), 1057–1067. https://doi.org/10.1007/s00468-017-1530-x.
Geoportal Berlin (2015) *Soil types*. https://fbinter.stadt-berlin.de/fb/ index.jsp [Accessed 8 August 2023].
Gessler, A., Bächli, L., Rouholahnejad Freund, E., Treydte, K., Schaub, M., Haeni, M., et al., 2022. Drought reduces water uptake in beech from the drying topsoil, but no compensatory uptake occurs from deeper soil layers. New Phytol. 233 (1), 194–206. https://doi.org/10.1111/nph.17767.
Gessner, M.O., Hinkelmann, R., Nützmann, G., Jekel, M., Singer, G., Lewandowski, J., et al., 2014. Urban water interfaces. J. Hydrol. 514, 226–232. https://doi.org/10.1016/j.jhydrol.2014.04.021.
Gillefalk, M., Tetzlaff, D., Hinkelmann, R., Kuhlemann, L.-M., Smith, A., Meier, F., et al., 2021. Quantifying the effects of urban green space on water partitioning and ages using an isotope-based ecohydrological model. Hydrol. Earth Syst. Sci. 25 (6), 3635–3652. https://doi.org/10.5194/hess-25-3635-2021.
Gillefalk, M., Tetzlaff, D., Marx, C., Smith, A., Meier, F., Hinkelmann, R., et al., 2022. Estimates of water partitioning in complex urban landscapes with isotope-aided ecohydrological modelling. Hydrol. Process. 36 (3) https://doi.org/10.1002/hyp.14532.
Gillner, S., Bräuning, A., Roloff, A., 2014. Dendrochronological analysis of urban trees: climatic response and impact of drought on frequently used tree species. Trees 28 (4), 1079–1093. https://doi.org/10.1007/s00468-014-1019-9.
Gillner, S., Korn, S., Roloff, A., 2015a. Leaf-gas exchange of five tree species at urban street sites. Arboricult. Urban For. 41 (3). https://doi.org/10.48044/jauf.2015.012.
Gillner, S., Vogt, J., Tharang, A., Dettmann, S., Roloff, A., 2015b. Role of street trees in mitigating effects of heat and drought at highly sealed urban sites. Landsc. Urban Plan. 143, 33–42. https://doi.org/10.1016/j.landurbplan.2015.06.005.
Gillner, S., Korn, S., Hofmann, M., Roloff, A., 2017. Contrasting strategies for tree species to cope with heat and dry conditions at urban sites. Urban Ecosystems 20 (4), 853–865. https://doi.org/10.1007/s11252-016-0636-z.
Gillner, S., Fenner, D., Bräuning, A., Rohde, M., Roloff, A., Seliger, S.-W., Anja, et al., 2020. Response of growth to climate within oaks of the world heritage site of prussian gardens. Int. J. Forestry Horticulture 6 (2). https://doi.org/10.20431/2454-9487.0602001.
Gómez-Navarro, C., Pataki, D.E., Bowen, G.J., Oerter, E.J., 2019. Spatiotemporal variability in water sources of urban soils and trees in the semiarid, irrigated salt Lake Valley. Ecohydrology 12 (8). https://doi.org/10.1002/eco.2154.
Grimm, N.B., Faeth, S.H., Golubiewski, N.E., Redman, C.L., Wu, J., Bai, X., et al., 2008. Global Change and the Ecology of Cities. *Science* 319, 756–760.
Guo, D., 2022. Modelling actual, potential and reference crop: package 'evapotranspiration'. Accessed 30 March 2023. https://cran.rstudio.com/web/packages/Evapotranspiration/Evapotranspiration.pdf.
Gutiérrez, E., Campelo, F., Camarero, J.J., Ribas, M., Muntán, E., Nabais, C., et al., 2011. Climate controls act at different scales on the seasonal pattern of Quercus ilex L. stem radial increments in NE Spain. Trees 25 (4), 637–646. https://doi.org/10.1007/s00468-011-0540-3.
Haase, D., Hellwig, R., 2022. Effects of heat and drought stress on the health status of six urban street tree species in Leipzig, Germany. Trees, Forests and People 8, 100252. https://doi.org/10.1016/j.tfp.2022.100252.
Hao, G.-Y., Wheeler, J.K., Holbrook, N.M., Goldstein, G., 2013. Investigating xylem embolism formation, refilling and water storage in tree trunks using frequency domain reflectometry. J. Exp. Bot. 64 (8), 2321–2332. https://doi.org/10.1093/jxb/ert090.
Herrmann, V., McMahon, S.M., Detto, M., Lutz, J.A., Davies, S.J., Chang-Yang, C.-H., et al., 2016. Tree circumference dynamics in four forests characterized using automated dendrometer bands. PLoS One 11 (12), e0169020.
Hodnebrog, Ø., Marelle, L., Alterskjær, K., Wood, R.R., Ludwig, R., Fischer, E.M., et al., 2019. Intensification of summer precipitation with shorter time-scales in Europe. Environ. Res. Lett. 14 (12), 124050 https://doi.org/10.1088/1748-9326/ab549c.
Hughes, C.E., Crawford, J., 2012. A new precipitation weighted method for determining the meteoric water line for hydrological applications demonstrated using australian and global GNIP data. J. Hydrol. 464–465, 344–351. https://doi.org/10.1016/j.jhydrol.2012.07.029.
Ipcc, 2023. Climate Change 2022 – Impacts. Cambridge University Press, Adaptation and Vulnerability.
Khair, Z.M.E., Joly, L., Cousin, J., Decarpenterie, T., Dumelié, N., Maamary, R., et al., 2017. In situ measurements of methane in the troposphere and the stratosphere by the ultra light SpEctrometer amulse. Appl. Phys. B 123 (12). https://doi.org/10.1007/s00340-017-6850-4.
Kleine, L., Tetzlaff, D., Smith, A., Wang, H., Soulsby, C., 2020. Using water stable isotopes to understand evaporation, moisture stress, and re-wetting in catchment forest and grassland soils of the summer drought of 2018. Hydrol. Earth Syst. Sci. 24 (7), 3737–3752. https://doi.org/10.5194/hess-24-3737-2020.
Kowarik, I. (2011) Novel urban ecosystems, biodiversity, and conservation. *Environmental Pollution (Barking, Essex : 1987)*, 159(8-9), 1974–1983. https://doi.org/10.1016/j.envpol.2011.02.022.
Kruskal, W.H., Wallis, W.A., 1952. Use of ranks in one-criterion variance analysis. J. Am. Stat. Assoc. 47 (260), 583. https://doi.org/10.2307/2280779.
Kübert, A., Dubbert, M., Bamberger, I., Kühnhammer, K., Beyer, M., van Haren, J., et al., 2022. Tracing plant source water dynamics during drought by continuous transpiration measurements: an in-situ stable isotope approach. Plant Cell Environ. 46 (1), 133–149. https://doi.org/10.1111/pce.14475.
Kuhlemann, L.-M., Tetzlaff, D., Smith, A., Kleinschmit, B., Soulsby, C., 2021. Using soil water isotopes to infer the influence of contrasting urban green space on ecohydrological partitioning. Hydrol. Earth Syst. Sci. 25 (2), 927–943. https://doi.org/10.5194/hess-25-927-2021.
Kühnhammer, K., Dahlmann, A., Iraheta, A., Gerchow, M., Birkel, C., Marshall, J.D., et al., 2022. Continuous in situ measurements of water stable isotopes in soils, tree trunk and root xylem: field approval. Rapid Commun. Mass Spectrom. 36 (5), e9232.
Kühnhammer, K., van Haren, J., Kübert, A., Bailey, K., Dubbert, M., Hu, J., et al., 2023. Deep roots mitigate drought impacts on tropical trees despite limited quantitative contribution to transpiration. Sci. Total Environ. 893, 164763 https://doi.org/10.1016/j.scitotenv.2023.164763.
Kunz, J., Räder, A., Bauhus, J., 2016. Effects of drought and rewetting on growth and gas exchange of minor european broadleaved tree species. Forests 7 (12), 239. https://doi.org/10.3390/f7100239.
Landgraf, J., Tetzlaff, D., Dubbert, M., Dubbert, D., Smith, A., Soulsby, C., 2022. Xylem water in riparian willow trees (Salix alba) reveals shallow sources of root water uptake by in situ monitoring of stable water isotopes. Hydrol. Earth Syst. Sci. 26 (8), 2073–2092. https://doi.org/10.5194/hess-26-2073-2022.
Landwehr, J.M. & Coplen, T. (2006) *Line-conditioned excess: a new method for characterizing stable hydrogen and oxygen isotope ratios in hydrologic systems*.
Lanning, M., Wang, L., Benson, M., Zhang, Q., Novick, K.A., 2020. Canopy isotopic investigation reveals different water uptake dynamics of maples and oaks. Phytochemistry 175, 112389. https://doi.org/10.1016/j.phytochem.2020.112389.
Leipzig, U.F.Z., 2023. Drought monitor Germany. Accessed 8 August 2023. https://www.ufz.de/index.php?de=37937#:~:text=Die%20Rechte%20der%20Grafiken%20und,%2F%20Helmholtz%2DZentrum%20f%C3%BCr%20Umweltforschung.
Limberg, A., Darkow, P., Faensen-Thiebes, A., Fritz-Taute, B., Günther, M., Hähnel, K., et al., 2007. Grundwasser in Berlin, vorkommen·nutzung·schutz·gefährdung. – senatsverwaltung für gesundheit. Umwelt und Verbraucherschutz, Berlin [Accessed 8 August 2023].
Limberg, A., Thierbach, J., 2002. Hydrostratigrafie von Berlin-korrelation mit dem norddeutschen gliederungsschema. Brandenburgische Geowissenschaftliche Beiträge 2002, 65–68.
Litvak, E., Manago, K.F., Hogue, T.S., Pataki, D.E., 2017. Evapotranspiration of urban landscapes in L os a ngeles, C alifornia at the municipal scale. Water Resour. Res. 53 (5), 4236–4252. https://doi.org/10.1002/2016WR020254.
Liu, Y., Ju, W., Chen, J., Zhu, G., Xing, B., Zhu, J., et al., 2012. Spatial and temporal variations of forest LAI in China during 2000–2010. Chin. Sci. Bull. 57 (22), 2846–2856. https://doi.org/10.1007/s11434-012-5064-8.
Livesley, S.J., McPherson, G.M., Calfapietra, C., 2016. The urban Forest and ecosystem services: impacts on urban water, heat, and pollution cycles at the tree, street, and City scale. J. Environ. Qual. 45 (1), 119–124. https://doi.org/10.2134/jeq2015.11.0567.
Majoube, M., 1971. Fractionnement en oxygène 18 et en deutérium entre l'eau et sa vapeur. J. Chim. Phys. 68, 1423–1436. https://doi.org/10.1051/jcp/1971681423.
Mann, H.B., Whitney, D.R., 1947. On a test of whether one of two random variables is stochastically larger than the other. Ann. Math. Stat. 18 (1), 50–60. https://doi.org/10.1214/AOMS%2F1177730491.
Marchin, R.M., Esperon-Rodriguez, M., Tjoelker, M.G., Ellsworth, D.S., 2022. Crown dieback and mortality of urban trees linked to heatwaves during extreme drought. Sci. Total Environ. 850, 157915 https://doi.org/10.1016/j.scitotenv.2022.157915.
Marshall, J.D., Cuntz, M., Beyer, M., Dubbert, M., Kuehnhammer, K., 2020. Borehole equilibration: testing a new method to monitor the isotopic composition of tree xylem water in situ. Front. Plant Sci. 11, 358. https://doi.org/10.3389/fpls.2020.00358.
Marshall, D.C. (1958) *Measurement of sap flow in conifers by heat transport.*
Martín-Gómez, P., Aguilera, M., Pemán, J., Gil-Pelegrín, E., Ferrio, J.P., 2016. Contrasting ecophysiological strategies related to drought: the case of a mixed stand of scots pine (Pinus sylvestris) and a submediterranean oak (quercus subpyrenaica). Tree Physiol. 37 (11), 1478–1492. https://doi.org/10.1093/treephys/tpx101.
Marx, C., Tetzlaff, D., Hinkelmann, R., Soulsby, C., 2022. Seasonal variations in soil–plant interactions in contrasting urban green spaces: insights from water stable isotopes. J. Hydrol. 612, 127998 https://doi.org/10.1016/j.jhydrol.2022.127998.
McGrane, S.J., 2016. Impacts of urbanisation on hydrological and water quality dynamics, and urban water management: a review. Hydrol. Sci. J. 61 (13), 2295–2311. https://doi.org/10.1080/02626667.2015.1128084.
McLaughlin, S.B., Wullschleger, S.D., Nosal, M., 2003. Diurnal and seasonal changes in stem increment and water use by yellow poplar trees in response to environmental stress. Tree Physiol. 23 (16), 1125–1136. https://doi.org/10.1093/treephys/23.16.1125.
Meili, N., Manoli, G., Burlando, P., Carmeliet, J., Chow, W.T., Coutts, A.M., et al., 2021. Tree effects on urban microclimate: diurnal, seasonal, and climatic temperature differences explained by separating radiation, evapotranspiration, and roughness effects. Urban For. Urban Green. 58, 126970 https://doi.org/10.1016/j.ufug.2020.126970.
T. Meinert, C. Frühauf, B. Plückhahn, A. Brömser, (2022) Die Trockenheit in Deutschland im Sommer 2022 aus agrarmeteorologischer Sicht. https://www.dwd.de/DE/leistungen/besondereereignisse/duerre/20220811_trockenheit_sommer_2022.pdf?__blob=publicationFile&v=2.
Mendes de Moura, Y., Hilker, T., Lyapustin, A.I., Galvão, L.S., dos Santos, J.R., Anderson, L.O., et al., 2015. Seasonality and drought effects of amazonian forests observed from multi-angle satellite data. Remote Sens. Environ. 171, 278–290. https://doi.org/10.1016/j.rse.2015.10.015.
Mennekes, D., Rinderer, M., Seeger, S., Orlowski, N., 2021. Ecohydrological travel times derived from in situ stable water isotope measurements in trees during a semi-controlled pot experiment. Hydrol. Earth Syst. Sci. 25 (8), 4513–4530. https://doi.org/10.5194/hess-25-4513-2021.

Myhre, G., Alterskjær, K., Stjern, C.W., Hodnebrog, Ø., Marelle, L., Samset, B.H., et al., 2019. Frequency of extreme precipitation increases extensively with event rareness under global warming. Sci. Rep. 9 (1), 16063. https://doi.org/10.1038/s41598-019-52277-4.

Nehemy, M.F., Millar, C., Janzen, K., Gaj, M., Pratt, D.L., Laroque, C.P., et al., 2019. 17 O-excess as a detector for co-extracted organics in vapor analyses of plant isotope signatures. Rapid Commun. Mass Spectrom. 33 (16), 1301–1310. https://doi.org/10.1002/rcm.8470.

Nowak, D.J., Dwyer, J.F., 2007. Understanding the benefits and costs of urban Forest ecosystems. In: Kuser, J.E. (Ed.), Urban and Community Forestry in the Northeast. Springer, Netherlands, Dordrecht, pp. 25–46.

Oke, T.R., 1982. The energetic basis of the urban heat island. Q. J. R. Meteorolog. Soc. 108 (455), 1–24. https://doi.org/10.1002/qj.49710845502.

Oren, R., Phillips, N., Ewers, B.E., Pataki, D.E., Megonigal, J.P., 1999. Sap-flux-scaled transpiration responses to light, vapor pressure deficit, and leaf area reduction in a flooded Taxodium distichum forest. Tree Physiol. 19 (6), 337–347. https://doi.org/10.1093/treephys/19.6.337.

Oswald, C.J., Kelleher, C., Ledford, S.H., Hopkins, K.G., Sytsma, A., Tetzlaff, D., et al., 2023. Integrating urban water fluxes and moving beyond impervious surface cover: a review. J. Hydrol. 618, 129188 https://doi.org/10.1016/j.jhydrol.2023.129188.

Papasozomenou, O., Moss, T., García Soler, N., 2019. Raindrops keep falling on my roof: imaginaries, infrastructures and institutions shaping rainwater harvesting in Berlin. J. Environ. Plann. Policy Manage. 21 (4), 358–372. https://doi.org/10.1080/1523908X.2019.1623658.

E. Paton J. Vogel B. Kluge T. Nehls Ausmaß 2021 Extent, trend and extremes of droughts in urban areas Trend und Extrema von Dürren im urbanen Raum 10.5675/HyWa_2021.1_1.

Pauleit, S. (2003) Urban street tree plantings: identifying the key requirements. *Proceedings of the Institution of Civil Engineers - Municipal Engineer*, 156(1), 43–50. https://doi.org/10.1680/muen.2003.156.1.43.

Peng, S., Piao, S., Ciais, P., Friedlingstein, P., Ottle, C., Bréon, F.-M., et al., 2012. Surface urban heat island across 419 global big cities. Environ. Sci. Tech. 46 (2), 696–703. https://doi.org/10.1021/es2030438.

Ponte, S., Sonti, N.F., Phillips, T.H., Pavao-Zuckerman, M.A., 2021. Transpiration rates of red maple (Acer rubrum L.) differ between management contexts in urban forests of Maryland, USA. Sci. Rep. 11 (1), 22538. https://doi.org/10.1038/s41598-021-01804-3.

Preisler, Y., Hölttä, T., Grünzweig, J.M., Oz, I., Tatarinov, F., Ruehr, N.K., et al., 2022. The importance of tree internal water storage under drought conditions. Tree Physiol. 42 (4), 771–783. https://doi.org/10.1093/treephys/tpab144.

Rakovec, O., Samaniego, L., Hari, V., Markonis, Y., Moravec, V., Thober, S., et al., 2022. The 2018–2020 multi-year drought sets a new benchmark in Europe. earth's. Future 10 (3). https://doi.org/10.1029/2021EF002394.

Rocha, E., Holzkämper, S., 2023. Assessing urban climate effects on Pinus sylvestris with point dendrometers: a case study from Stockholm. Sweden. *Trees* 37 (1), 31–40. https://doi.org/10.1007/s00468-020-02082-8.

Rötzer, T., Moser-Reischl, A., Rahman, M.A., Hartmann, C., Paeth, H., Pauleit, S., et al., 2021. Urban tree growth and ecosystem services under extreme drought. Agric. For. Meteorol. 308–309, 108532 https://doi.org/10.1016/j.agrformet.2021.108532.

Roy, S., Byrne, J., Pickering, C., 2012. A systematic quantitative review of urban tree benefits, costs, and assessment methods across cities in different climatic zones. Urban For. Urban Green. 11 (4), 351–363. https://doi.org/10.1016/j.ufug.2012.06.006.

Saher, R., Stephen, H., Ahmad, S., 2020. Urban evapotranspiration of green spaces in arid regions through two established approaches: a review of key drivers, advancements, limitations, and potential opportunities. Urban Water J. 18 (2), 115–127. https://doi.org/10.1080/1573062X.2020.1857796.

Sánchez-Costa, E., Poyatos, R., Sabaté, S., 2015. Contrasting growth and water use strategies in four co-occurring Mediterranean tree species revealed by concurrent measurements of sap flow and stem diameter variations. Agric. For. Meteorol. 207, 24–37. https://doi.org/10.1016/j.agrformet.2015.03.012.

Seeger, S., Weiler, M., 2021. Temporal dynamics of tree xylem water isotopes: in situ monitoring and modeling. Biogeosciences 18 (15), 4603–4627. https://doi.org/10.5194/bg-18-4603-2021.

SEnSBW (2022) *StEP Klima 2.0*. https://www.berlin.de/sen/stadtentwicklung/planung/stadtentwicklungsplaene/step-klima-2-0/ [Accessed 8 August 2023].

SenUVK, 2019a. Grünflächeninformationssystem (GRIS): anteil öffentlicher grünflächen in Berlin. Accessed 10 August 2020. https://www.berlin.de/senuvk/umwelt/stadtgruen/gruenanlagen/de/daten_fakten/downloads/ausw_5.pdf.

SenUVK, 2019b. Grünflächeninformationssystem (GRIS): öffentliche grünflächen in Berlin – flächenübersicht der bezirke. Accessed 30 March 2023. https://www.berlin.de/sen/uvk/_assets/natur-gruen/stadtgruen/daten-und-fakten/ausw_13.pdf.

Shapiro, S.S., Wilk, M.B., 1965. An analysis of variance test for normality (complete samples). Biometrika 52 (3/4), 591. https://doi.org/10.2307/2333709.

Shashua-Bar, L., Pearlmutter, D., Erell, E., 2011. The influence of trees and grass on outdoor thermal comfort in a hot-arid environment. Int. J. Climatol. 31 (10), 1498–1506. https://doi.org/10.1002/joc.2177.

Siehr, S.A., Sun, M., Aranda Nucamendi, J.L., 2022. Blue-green infrastructure for climate resilience and urban multifunctionality in chinese cities. WIREs. Energy Environ. 11 (5) https://doi.org/10.1002/wene.447.

Smith, D., Jarvis, P.G., Odongo, J.C., 1997. Sources of water used by trees and millet in sahelian windbreak systems. J. Hydrol. 198 (1–4), 140–153. https://doi.org/10.1016/S0022-1694(96)03311-2.

Smith, A., Tetzlaff, D., Landgraf, J., Dubbert, M., Soulsby, C., 2022a. Modelling temporal variability of in situ soil water and vegetation isotopes reveals ecohydrological couplings in a riparian willow plot. Biogeosciences 19 (9), 2465–2485. https://doi.org/10.5194/bg-19-2465-2022.

Smith, A.A., Tetzlaff, D., Maneta, M., Soulsby, C., 2022b. Critical zone response times and water age relationships under variable catchment wetness states: insights using a tracer-aided ecohydrological model. Water Resour. Res. 58 (4) https://doi.org/10.1029/2021WR030584.

Snelgrove, J.R., Buttle, J.M., Kohn, M.J., Tetzlaff, D., 2021. Co-evolution of xylem water and soil water stable isotopic composition in a northern mixed forest biome. Hydrol. Earth Syst. Sci. 25 (4), 2169–2186. https://doi.org/10.5194/hess-25-2169-2021.

Soulsby, C., Birkel, C., Tetzlaff, D., 2014. Assessing urbanization impacts on catchment transit times. Geophys. Res. Lett. 41 (2), 442–448. https://doi.org/10.1002/2013GL058716.

Spearman, C., 1904. "General intelligence," objectively determined and measured. Am. J. Psychol. 15 (2), 201. https://doi.org/10.2307/1412107.

Sprenger, M., Tetzlaff, D., Soulsby, C., 2017. Soil water stable isotopes reveal evaporation dynamics at the soil–plant–atmosphere interface of the critical zone. Hydrol. Earth Syst. Sci. 21 (7), 3839–3858. https://doi.org/10.5194/hess-21-3839-2017.

Sprenger, M., Stumpp, C., Weiler, M., Aeschbach, W., Allen, S.T., Benettin, P., et al., 2019. The demographics of water: a review of water ages in the critical zone. Rev. Geophys. 57 (3), 800–834. https://doi.org/10.1029/2018RG000633.

Stevenson, J.L., Birkel, C., Comte, J.-C., Tetzlaff, D., Marx, C., Neill, A., et al., 2023. Quantifying heterogeneity in ecohydrological partitioning in urban green spaces through the integration of empirical and modelling approaches. Environ. Monit. Assess. 195 (4), 468. https://doi.org/10.1007/s10661-023-11055-6.

Suleiman, L., Olofsson, B., Saurí, D., Palau-Rof, L., García Soler, N., Papasozomenou, O., et al., 2020. Diverse pathways—common phenomena: comparing transitions of urban rainwater harvesting systems in Stockholm, Berlin and Barcelona. J. Environ. Plan. Manag. 63 (2), 369–388. https://doi.org/10.1080/09640568.2019.1589432.

Szymczak, S., Häusser, M., Garel, E., Santoni, S., Huneau, F., Knerr, I., et al., 2020. How do Mediterranean pine trees respond to drought and precipitation events along an elevation gradient? Forests 11 (7), 758. https://doi.org/10.3390/f11070758.

Tams, L., Paton, E.N., Kluge, B., 2023. Impact of shading on evapotranspiration and water stress of urban trees. Ecohydrology. https://doi.org/10.1002/eco.2556.

Tetzlaff, D., Buttle, J., Carey, S.K., McGuire, K., Laudon, H., Soulsby, C., 2015. Tracer-based assessment of flow paths, storage and runoff generation in northern catchments: a review. Hydrol. Process. 29 (16), 3475–3490. https://doi.org/10.1002/hyp.10412.

Tetzlaff, D., Buttle, J., Carey, S.K., Kohn, M.J., Laudon, H., McNamara, J.P., et al., 2021. Stable isotopes of water reveal differences in plant – soil water relationships across northern environments. Hydrol. Process. 35 (1) https://doi.org/10.1002/hyp.14023.

Vega-Grau, A.M., McDonnell, J., Schmidt, S., Annandale, M., Herbohn, J., 2021. Isotopic fractionation from deep roots to tall shoots: a forensic analysis of xylem water isotope composition in mature tropical savanna trees. Sci. Total Environ. 795, 148675 https://doi.org/10.1016/j.scitotenv.2021.148675.

Volkmann, T.H.M., Kühnhammer, K., Herbstritt, B., Gessler, A., Weiler, M., 2016. A method for in situ monitoring of the isotope composition of tree xylem water using laser spectroscopy. Plant Cell Environ. 39 (9), 2055–2063. https://doi.org/10.1111/pce.12725.

von Freyberg, J., Allen, S.T., Grossiord, C., Dawson, T.E., 2020. Plant and root-zone water isotopes are difficult to measure, explain, and predict: some practical recommendations for determining plant water sources. Methods Ecol. Evol. 11 (11), 1352–1367. https://doi.org/10.1111/2041-210X.13461.

Vulova, S., Rocha, A.D., Meier, F., Nouri, H., Schulz, C., Soulsby, C., et al., 2023. City-wide, high-resolution mapping of evapotranspiration to guide climate-resilient planning. Remote Sens. Environ. 287, 113487 https://doi.org/10.1016/j.rse.2023.113487.

Wassenaar, L.I., Hendry, M.J., Chostner, V.L., Lis, G.P., 2008. High resolution pore water delta2H and delta18O measurements by H2O(liquid)-H2O(vapor) equilibration laser spectroscopy. Environ. Sci. Tech. 42 (24), 9262–9267. https://doi.org/10.1021/es802065s.

Wen, M., He, D., Li, M., Ren, R., Jin, J., Si, B., 2022. Causes and factors of cryogenic extraction biases on isotopes of xylem water. Water Resour. Res. 58 (8) https://doi.org/10.1029/2022WR032182.

Wilcoxon, F., 1945. Individual comparisons by ranking methods. Biometrics 1 (6), 80. https://doi.org/10.2307/3001968.

Willis, K.J., Petrokofsky, G., 2017. The natural capital of city trees. Science (New York, N.Y.) 356 (6336), 374–376. https://doi.org/10.1126/science.aam9724.

Wouters, H., De Ridder, K., Poelmans, L., Willems, P., Brouwers, J., Hosseinzadehtalaei, P., et al., 2017. Heat stress increase under climate change twice as large in cities as in rural areas: a study for a densely populated midlatitude maritime region. Geophys. Res. Lett. 44 (17), 8997–9007. https://doi.org/10.1002/2017GL074889.

Yakir, D., Sternberg, L.S.L., 2000. The use of stable isotopes to study ecosystem gas exchange. Oecologia 123 (3), 297–311. https://doi.org/10.1007/s004420051016.

Zhang, Q., Jia, X., Shao, M., Zhang, C., Li, X., Ma, C., 2018. Sap flow of black locust in response to short-term drought in southern loess plateau of China. Sci. Rep. 8 (1), 6222. https://doi.org/10.1038/s41598-018-24669-5.

Zhao, L., Wang, L., Cernusak, L.A., Liu, X., Xiao, H., Zhou, M., et al., 2016. Significant difference in hydrogen isotope composition between xylem and tissue water in populus euphratica. Plant Cell Environ. 39 (8), 1848–1857. https://doi.org/10.1111/pce.12753.

Zweifel, R., Zimmermann, L., Newbery, D.M., 2005. Modeling tree water deficit from microclimate: an approach to quantifying drought stress. Tree Physiol. 25 (2), 147–156. https://doi.org/10.1093/treephys/25.2.147.